Application of Improved Detailed Hydrological Model:

Linking Groundwater and Surface Water in esker-peatland hydrological formation

Lassi Päkkilä[2], Meseret Menberu[1], Anna Autio[2], Hannu Marttila[2], Anna-Kaisa Ronkanen[1,2], Noora Veijalainen[1], Markus Huttunen[1]

[1]Finnish Environment Institute, Helsinki, Finland

[2]Water, Energy and Environmental Engineering Research Unit, University of Oulu, Oulu, Finland

Abstract

This study tested two different hydrological models, a semi-distributed conceptual national operational hydrological model (WSFS) developed by SYKE, and a fully integrated three-dimensional numerical model (HydroGeoSphere; HGS) in a typical Finnish heterogeneous environment and compared the results. The modelled catchments consist of an esker aquifer and its surrounding vast, groundwater fed peatlands, with several springs, streams, and groundwater fed lakes. The goal was to better understand groundwater and surface water interactions to facilitate brook and wetland restoration, to provide information on the importance of groundwater component on peatlands and in streamflow generation

The HGS model was not calibrated due to the model's complexity, limited input data, and limited resources, resulting in questionable results. Although simulated groundwater levels in a few wells and water levels in two lakes agreed better with their respective observed values, in general, HGS model results showed significant differences between simulated and observed values, making comparison with WSFS results difficult. The WSFS model, however, was calibrated from 2015 to 2020, and validated between 2021 and 2022 at four discharge observation stations. In spite of the short calibration and validation periods, the WSFS model achieved satisfactory fit between observed and simulated values as indicated by the Nash-Sutcliff model efficiency values (R^2) of both calibration (station i6000100q: $R^2 = 0.78$, station i6000110q: $R^2 = 0.66$, station i6000200q: $R^2 = 0.76$, and station i6000410q: $R^2 = 0.75$), and validation (station i6000100q: $R^2 = 0.42$, station i6000110q: $R^2 = 0.65$, station i6000200q: $R^2 = 0.65$, and station i6000410q: $R^2 = 0.03$) periods.

The WSFS simulations showed frequent changes in soil moisture during spring, summer, and autumn, while the HGS simulations did not. Furthermore, the observed remote sensing soil moisture data from the SMOS satellite was better correlated with the WSFS simulated upper layer soil moisture than the HGS model. A lower hydraulic conductivity and higher bulk density in the bottom layer resulted in lower soil moisture values and amplitude in WSFS simulations, while HGS simulations showed unrealistically large soil moisture values and minimal fluctuations. In contrast to soil moisture comparisons, HGS simulated groundwater storage gain agreed somewhat with WSFS in the early simulation years, but they differed significantly in the later simulation years. The WSFS and HGS evapotranspiration values followed a similar pattern despite significant differences in the simulated evapotranspiration by the two models.

Overall, the WSFS model produced better results than the HGS model, primarily because the HGS model was not calibrated; hence, comparing the two models under these conditions was unrealistic. However, we have learned how powerful and realistic three-dimensional hydrological models can be, and we are aiming to enhance our simple WSFS model into a more physics-based one by integrating other three-dimensional models, such as MODFLOW, or by improving its conceptual equations.

LIFE14 IPE/FI00023 FRESHABIT LIFE IP

The project has received funding from the LIFE Programme of the European Union. The material reflects the views by the authors, and the European Commission or the CINEA is not responsible for any use that may be made of the information it contains.

1 Introduction

Hydrology, which studies water dynamics on the earth, is extremely important to the environment and to humans (Te Chow, 2010). Modelling hydrological systems is critical for a variety of applications, including planning for water resources, developing management methods, predicting floods, and integrating climate, hydrology, and the environment (Pechlivanidis et al., 2011). There has been continuous alteration of hydrologic systems due to rapid urbanization, industrialization (such as deforestation, land cover change, irrigation, etc.) and climate change (Devia et al., 2015). Hence, a wide variety of hydrological models have been developed to provide insight into hydrological processes in an increasingly changing environment that can be applied to very large basins. Hydrological models range from simple conceptual models e.g., HBV model (Seibert, 1997) to semi-distributed, such as; Soil & Water Assessment tool, SWAT; (Neitsch et al., 2011), Watershed Simulation and Forecasting System, WSFS (Huttunen et al., 2016; Jakkila et al., 2013; Vehviläinen & Huttunen, 2001) and complex fully-integrated surface and subsurface physically based models, e.g., HydroGeoSphere, HGS (Brunner & Simmons, 2012), and MIKE SHE (Graham & Butts, 2005).

A quantitative understanding of the hydrological cycle is becoming increasingly important as anthropogenic demands for water grow (Brunner & Simmons, 2012). Moreover, climate change and its subsequent impact on precipitation and infiltration, as well as the uncertainties associated with population growth, have made forecasting surface and groundwater supplies more difficult than ever (Li et al., 2008). The simulation of rainfall-runoff process in a catchment is among the most important hydrologic topics, and the use of simple conceptual models for the non-linear process can lead to errors (Gui et al., 2021). Traditional groundwater and surface water models neglect issues such as the integration of groundwater and surface water, the effects of surface water on groundwater and vice versa, the effects of land use changes and urban development on water resources, and the management of floodplains and wetlands (Graham & Butts, 2005). Furthermore, the demand for physically-based hydrologic models continues to rise as regulators and stakeholders recognize the importance of including regional-scale hydrologic budgets into groundwater management policies (Li et al., 2008). Hence, the use of fully integrated numerical hydrological models may provide a better understanding of catchment-scale hydrological processes (e.g., spatio-temporal interactions of groundwater and surface water, soil moisture, overland flow, sub-surface flow, etc.) than extremely simplified conceptual hydrological models.

Many ecosystems depend on groundwater: groundwater can provide important baseflow for streams and rivers, or feed lakes and peatlands. Changes in land use even outside the dependent ecosystems can influence the groundwater interactions. For example, many peatland habitat types in Finland have become endangered mainly due to extensive draining for forestry (Kontula & Raunio, 2018), and nutrient rich peatland types belong to the most endangered (Kaakinen et al. 2018). Nutrient-rich peatlands get their water not only through rain and snowmelt but as runoff and groundwater from the surrounding mineral soils (Kontula & Raunio, 2018; Similä et al., 2014); groundwater and runoff provide important nutrients, minerals and flow to peatlands. It is important to understand the hydrological interactions between peatlands and their surrounding areas to aid sustainable water use and the protection and restoration of these vulnerable ecosystems.

The main objectives are: 1) to test applicability of a three-dimensional fully integrated surface-subsurface hydrologic modelling tool (HydroGeoSphere; HGS) in a typical Finnish heterogenous catchment containing forestry, forestry-drained and pristine peatlands, partly restored peatlands, and an unconfined esker of soil types containing sand, gravel, and boulders. 2) using the HGS and national operational hydrological (WSFS) models, quantify the spatial-temporal soil moisture dynamics of the watershed under different land uses and soil types and compare the results. 3) propose suggestions or improvements, and best practices to the WSFS model by analyzing the required inputs and parameters for the two hydrologic models, as well as their limitations.

2 The HGS and WSFS Hydrologic Models

2.1 The Finnish Environment Institute's Hydrologic Model, the WSFS

The WSFS hydrological model is a semi-distributed, conceptual catchment model that was originally developed based on the HBV-model (Bergström, 1976), and later improved and modified by the Finnish Environment Institute to adapt to Finnish watershed conditions and requirements (Jakkila et al., 2013; Vehviläinen, 1991, 1992; Vehviläinen & Huttunen, 2001). The WSFS model consists of sub-models for areal precipitation, snow cover, soil moisture, groundwater, river routing, and lakes and is the main modeling tool used in flood forecasting in Finland (Jakkila et al., 2013).

The WSFS model describes the hydrologic processes in many subbasins in which each sub-basin is further divided into different soil and land use combinations (Figure 1). The soil and

land use combinations have a 1 km^2 grid cell size. In each grid cell, precipitation and temperature values are computed by interpolation using the nearest observation points, and then corrected for altitude difference between the stations and the grid cell. After daily precipitation and temperature are estimated for each grid cell, the rainfall-runoff model is simulated. The simulated runoff in each grid cell is then collected for each sub-basin and then routed using river models (Vehviläinen & Huttunen, 2002). Some of the algorithms in the WSFS model are still more conceptual than physical. However, the model is applied to a 1 km^2 grid size to produce high spatial distribution of hydrologic processes in a watershed. In the current WSFS model, soils in each land use class are divided into two-layers (upper layer: 10 cm – 20 cm, bottom layer: 80 cm – 100 cm thickness; Figure 1 b) and simulated in a daily time-step.

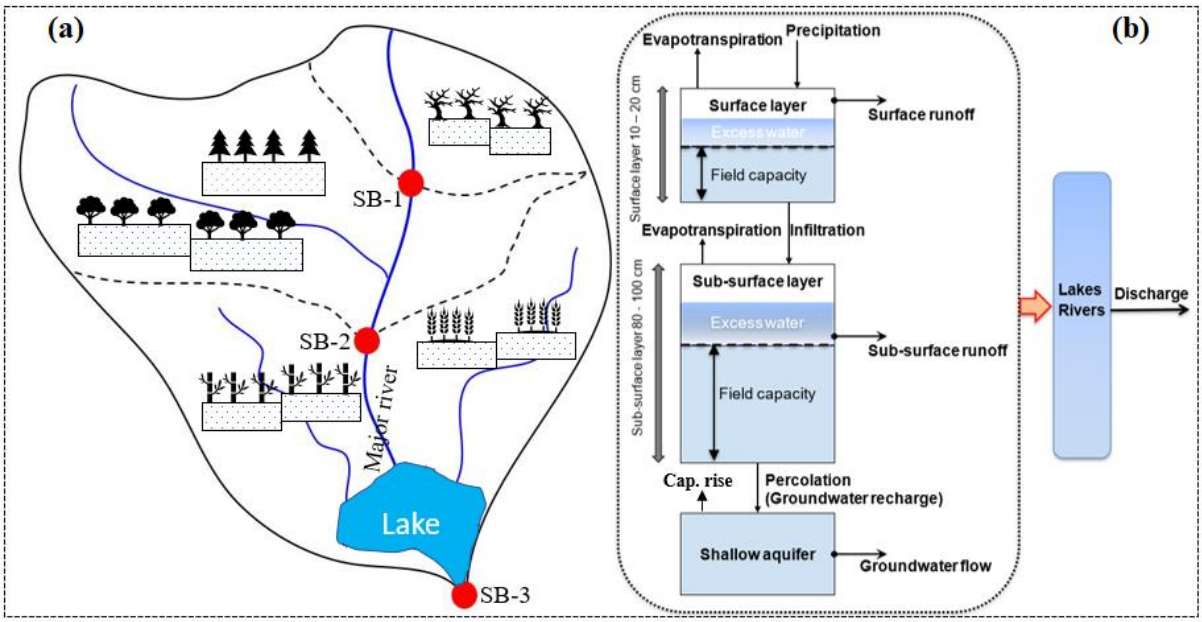

Figure 1. (a) schematics showing the input watershed for the WSFS model, its subbasins (SB-1, SB-2, SB-3) and their grid-cell classifications by soil type, vegetation, and elevation, (b) a two-layer soil moisture model with the major hydrologic processes for each soil-land-use class.

2.2 The HydroGeoSphere, HGS: Fully Integrated Surface-Subsurface Hydrologic Model

The HGS is a physically based, fully integrated surface and subsurface hydrologic model capable of simulating all hydrologic cycle components, including surface and subsurface flow processes, evapotranspiration, snow accumulation and snowmelt, and soil freezing/thawing, but also solute transport, all in three dimensions. There are several discretization options available in HGS, ranging from simple rectangular domains to irregular domains with complex geometry and layering.

The HGS simulates coupled surface and subsurface flows and transport using the control volume finite element method. The model solves both the modified Richard's equation and depth-integrated diffusion-wave approximation of the Saint Venant equation in a fully implicit manner for the three-dimensional unsaturated/saturated subsurface and two-dimensional surface water flow, respectively. The Hagen-Poiseuille analytic formula, Manning's formula, or Hazen-Williams empirical formula describe fluid flow in one-dimensional hydraulic features like streams, rivers, subsurface wells, and water supply lines. The HGS uses the conventional advection-dispersion equation for all domains involving solute or thermal energy transport (Aquanty, 2015; Brunner & Simmons, 2012).

In HGS, the concept of coupling length allows coupling the 1D flow domain and the 2D overland or 3D subsurface using the common node approach (continuity of hydraulic head between the domains) or dual node approach (first-order exchange coefficient) (Aquanty, 2015; Brunner & Simmons, 2012). From discretized flow and transport regimes, a single system of matrix equations is created for the entire hydrologic setting, with appropriate boundary conditions given to the combined system. Hence, at each time step, the linearized set of nonlinear discrete equations is solved simultaneously in an iterative manner using the Newton-Raphson technique (Aquanty, 2015; Brunner & Simmons, 2012).

Small-scale topographic variations can be accounted for in HGS using the concepts of rill storage and storage exclusion. Rill storage must be full before later surface flow can occur, and storage exclusion can count for reduced surface domain porosity, e.g., caused by buildings (Brunner & Simmons, 2012).

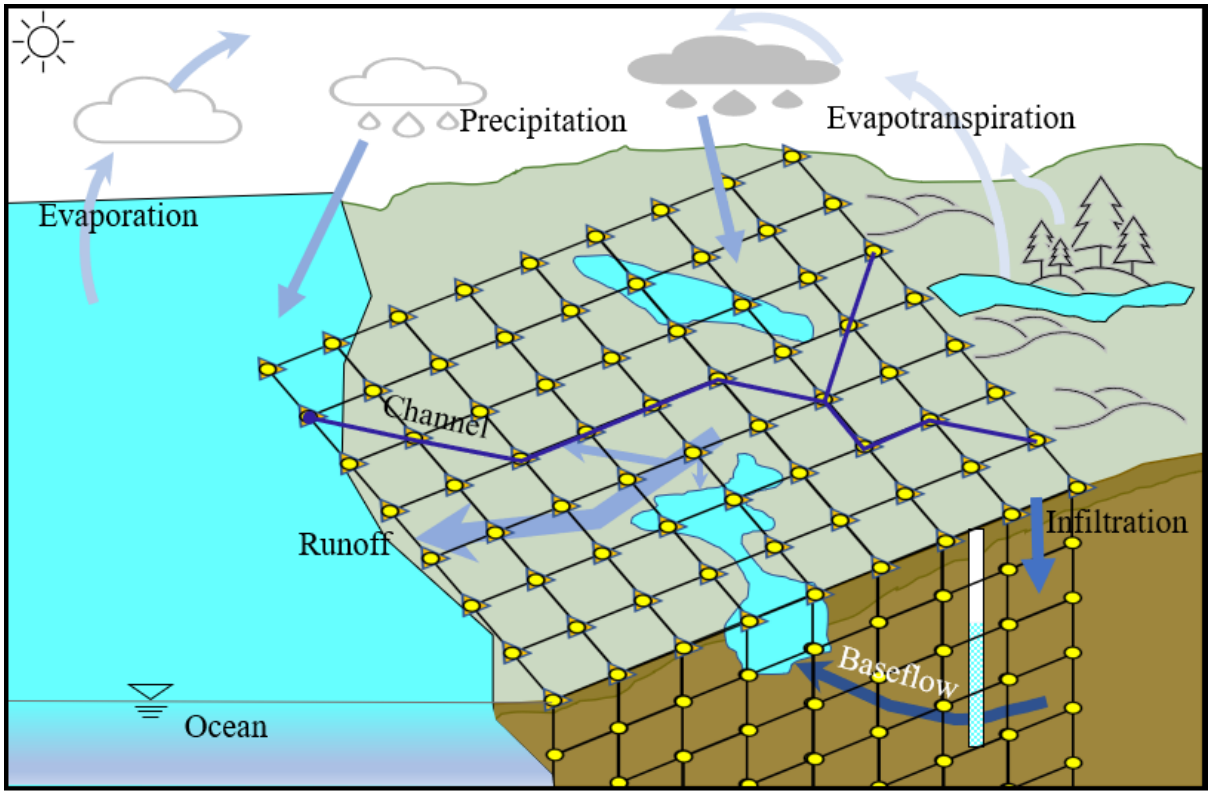

Figure 2. Simplified schematics showing Integrated Numerical Simulation of the Hydrologic System in HGS (Aquanty, 2015).

As shown in Figure 2, the coupled surface and subsurface domains of the HGS consist of (a) surface nodes shown by triangles situated on the land surface in a single layer (b) the vadose zone, subsurface aquifers, and aquitards shown by circles in the subsurface soil and aquifer node layers, and (c) surficial channels, wells, tile drains, storm and sanitary drains, water mains, and other linear features represented by a set of one-dimensional line elements, displayed as squares. Furthermore, to maintain surface topography and to ensure nodes in the surface grid coincide with the subsurface mesh nodes, a 2-D surface flow grid is draped over the 3-D subsurface mesh (Aquanty, 2015).

3 The Kiiminkijoki catchment WSFS and Kälväsvaara HydroGeoSphere models

3.1 A description of the test site and an overview of the two models

As part of the WSFS model delineation, the Kiiminkijoki catchment (watershed-id: 60) is located in Northern Ostrobothnia, Finland, and is further subdivided into nine second level and

59 third level subbasins (Figure 3). In the WSFS hydrological model, a daily time step simulation is performed according to scheme shown in Figure 1. In this model, evaporation is calculated for six different land use classes (coniferous forest, deciduous forest, fields, bog, open area and water) using the Penman-Monteith method. For the two-layer soil moisture model description of the WSFS, six soil classes are used (clay, silt, sand, organic, till, and rock). Based on the WSFS model delineation of the entire Kiiminkijoki catchment, the surface layer consists of 57% organic, 33% till, 7% sand, and 3% rock, while the subsurface layer consists of 40% organic, 36% till, 14% silt, 7% sand and 3%. There is an organic soil content ranging from 73-76% in each of the three subbasins (red boundary, Figure 3 a) within the Kiiminkijoki catchment, followed by sandy soil (9-21%), and till (7-18%) at the surface layer. The subsurface layer of these three subbasins contains organic (48-60%) and mineral soils such as sand (9-21%) and silt (15-22%). The parameters and their ranges used in the WSFS modelling are represented in Table 1.

The Kälväsvaara HydroGeoSphere (HGS) model boundary (shaded region in Figure 3 a) includes the Kälväsvaara unconfined esker aquifer (14.47 km^2 recharge area) and its adjacent vast aapa mire complexes, Leväsuo and Olvassuo and is inside the three red-colored subbasins of the main Kiiminkijoki catchment. Olvassuo aapa mire complex is mainly in pristine state but some of the margin parts have been drained for forestry in the 1960s and 70s (later partly restored in the 1990s and 2000s) (Heikkilä & Lindholm, 1997). Large parts of Olvassuo and Leväsuo mire complexes are part of the Natura 2000 protected areas network (SAC and SPA protection status), and a part of Olvassuo belongs to the Olvassuo Strict Nature Reserve. The peat thickness in the areas varies from a few tens of centimeteres in the margin areas close to Kälväsvaara to several meters in the wet center parts. The aquifer area consists of complex mixed layers of sand, gravel and boulders with lenses of glacial till and silt, underlain by a crystalline and possibly fractured bedrock. HGS modelled area includes several groundwater fed springs, groundwater fed lakes, ponds, and streams, both in peatland and in the aquifer area. Annual mean temperature in the area is around 1.5°C and annual aggregated precipitation varies between 500 and 600 mm (Isokangas et al., 2017). Annual evapotranspiration in the area is between 235 and 300 mm (Ala-aho et al., 2015). Hydrological properties (e.g., soil moisture, shallow groundwater storage, evaporation) of the shaded area and the shared area between the three subbasins were compared in two models (WSFS and HGS).

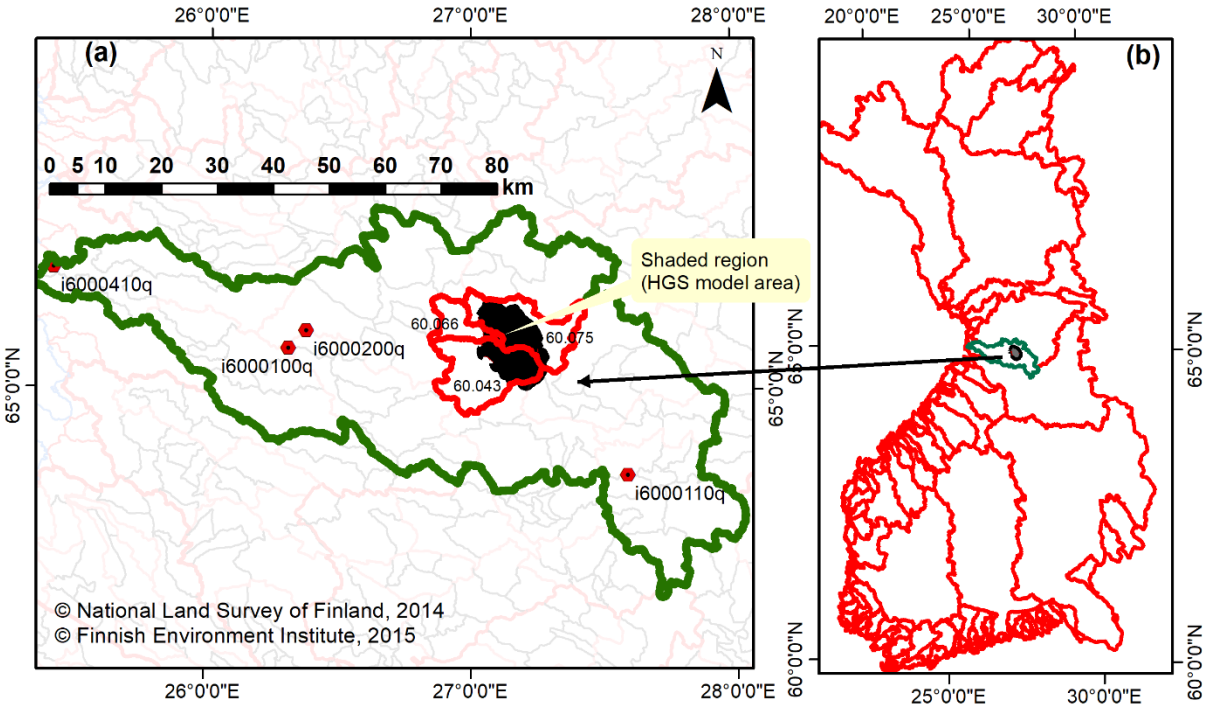

Figure 3. (a) WSFS's model first level catchment (green boundary), discharge observation points (i6000100q, i6000110q, i6000200q, i6000410q) and its sub-basins (transparent lines): red colored boundaries show third-level sub-basins (60.043 → 60_gv60_043, 60.066 → 60_gv60_066, and 60.075 → 60_gv60_075) that overlap with the shaded area modelled in HGS. (b) First level watersheds delineation in Finland used in the WSFS model.

The Kälväsvaara HGS model boundaries were selected to study the interaction of groundwater with the aquifer and surrounding peatland areas (Figure 4). Kälväsvaara is a large esker aquifer located in Northern Finland, in rural parts of Utajärvi municipality. It is a part of an esker ridge ranging in west-east direction from the Gulf of Bothnia to Suomussalmi in Eastern Finland, and reaches into about 200 meters above sea level at its highest point, and about 50 meters above the surrounding peatlands (Jaros et al., 2019). Modelling area limits into five larger lakes, Marttisjärvi, Iso Olvasjärvi, Pikku Olvasjärvi, Paskolampi, and Kärkkäänjärvi, and to river Piltuanjoki.

HGS modelling requires varying inputs to represent the modelling area accurately. Weather data (rain, snow depth, and temperature) data was downloaded from the Finnish Meteorological Institutes (FMI) grid interpolated weather data service since the modelling area did not have a weather station close by. Previously unpublished potential evapotranspiration (PET) data was kindly provided by the Finnish Meteorological Institute (Pirinen, 2021). PET data was

calculated with 1 km x 1 km grid interpolated weather data using the FAO Penman-Monteith equation (12 cm grass as reference crop) (Allen et al., 1998).

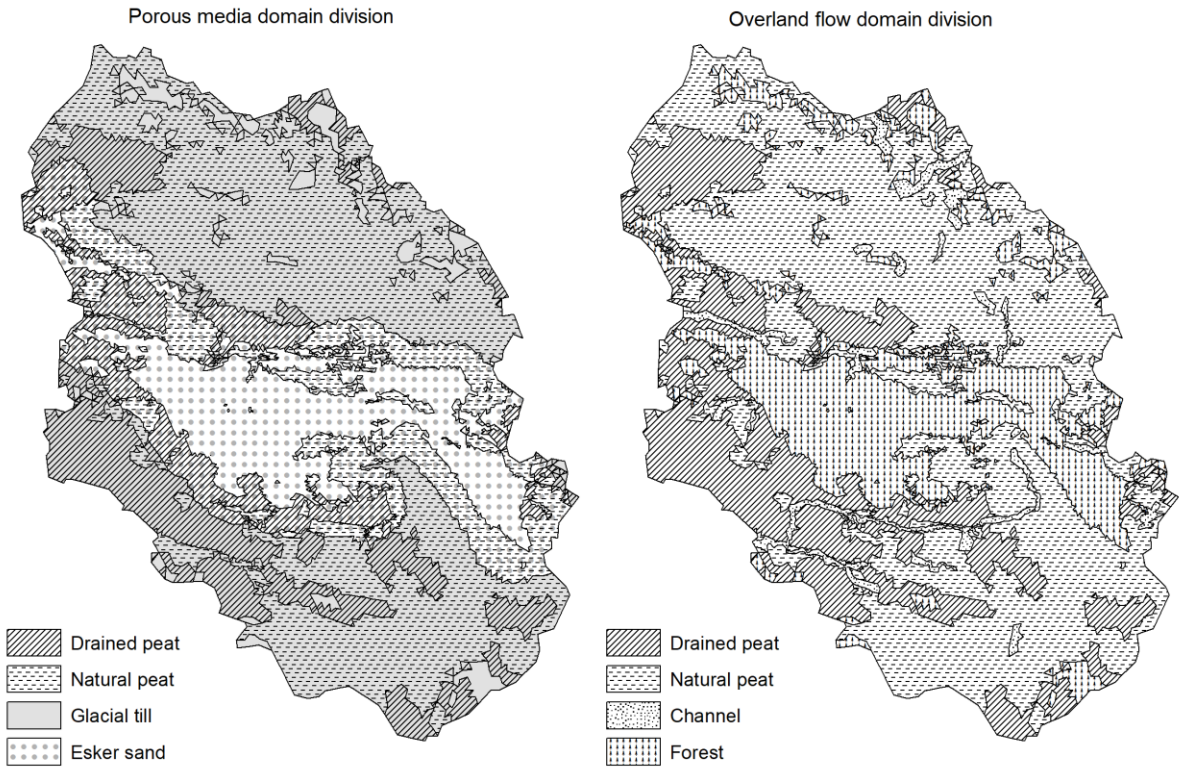

Figure 4. The Kälväsvaara HydroGeoSphere model area (shaded region in Figure 3) showing the porous media and overland flow domains.

A triangular element grid was generated for the HGS modelling area using AlgoMesh software (Figure 5). Observation wells, most in the esker area and some in the peatland areas were also added to the mesh. Mesh refinement and optimization resulted in a triangular element mesh of 11952 nodes and 23490 elements for the HGS model boundary (shaded region, Figure 3 a, Figure 5). The HGS model domain was divided into seven layers: surface to 0.05 m depth, 0.05 m to 0.1 m depth, 0.1 m to 0.25 m depth, 0.25 m to 0.667 m depth, 0.667 to 1.35 m depth (average peat depth), and from 1.35 m to the bedrock with two proportional layers (proportion of 34/66). Porous media properties, overland flow properties, and PET properties were assigned to the corresponding areas (Figure 4). Constant head boundary conditions were set to the nodes where model delimits into Kärkkäänjärvi, Marttisjärvi, Paskolampi, Iso Olvasjärvi, and Pieni Olvasjärvi. Long term average water levels of the lakes was used as input values (years 1989-2012, 19-68 measurements with 34 on average). A critical depth boundary condition was set to the whole surface domain.

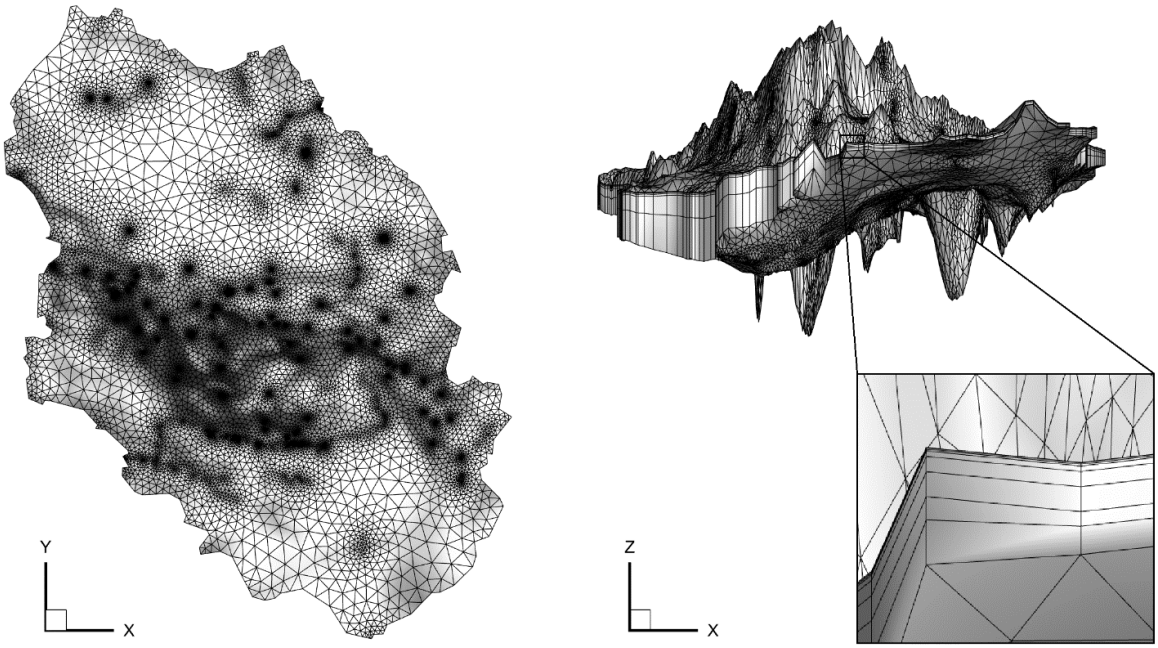

Figure 5. The triangular 2D mesh created in the Kälväsvaara HydroGeoSphere model area. In the channel areas and around observation points, the mesh is more refined.

The HGS was first run into steady state with output timesteps of 1, 2, 3, 5, 10, 20, 50, 100, 200, 500, and 1000 years. A dry surface was set with an initial water depth of 0.0001 meters. For the entire 1000-year period, effective rainfall was applied to the model to achieve steady state. The effective rainfall used was 315 mm/year, which equals the average annual precipitation (615 mm/year) minus the potential evapotranspiration of 300 mm/year, a typical value for Finland (Jaros et al., 2019). The PET properties used in the transient state models were not used in the steady state model, but rainfall and PET were applied in a lumped manner. Steady state run resulted a steady hydrological condition (heads and fluxes) for the area which could be used as an initial condition for transient run. The model was first transformed into transient state and run for the year 2016. Same porous media and overland flow properties were used in the model as in steady state. The PET, rainfall, and snowfall were applied to the area as time value tables, and daily timesteps were used as outputs. Rainfall was allowed to accumulate as snow in the spring (1.1-30.6.) and in the autumn (1.7.-31.12.) when daily average air temperature was below 2°C and 0°C, respectively. For the transient state 2015-2020 model, the 31st of December 2016 hydrological conditions were used as the initial head input. Again, same porous media, overland flow, and PET properties were used. Similarly, a time value table for the PET, rainfall, and snowfall was applied to the area, and the outputs were based on daily

timesteps. All the parameters different from HGS default parameters used in the HGS models are represented in Table 2.

HGS provides by default an overland flow and porous media solution, and a fluid mass balance for the model run. A range of other outputs are also available via specific commands and depending on the problem. The HGS runs were set up to produce soil water balance for the model domain. Soil water balance includes soil water volume, groundwater volume, top 0.1 m and top 1 m, total porous media, and surface water volumes. The previous and model area were used to calculate average soil moisture (m^3/m^3) in the top 0.1 m and 0.1 to 1 m layer. Total porous media water volume was transformed into porous groundwater storage in meters and millimeters. Daily groundwater storage change was then calculated by diminishing the daily value of groundwater storage by the average of the groundwater storage. HGS was also set to produce fluid mass balance output for specific areas using shapefiles. Shapefiles represent the different soil types in the area, which are drained peat, natural peat, esker sand, and glacial till, with the coverage of 23.79%, 56.70%, 16.27, and 3.24%, respectively. Combined total peat area of the model with drained and natural peat is 80.49%.

3.2 Required Data and Parameters for WSFS and HGS Models

Table 1. The parameters used in various processes of the WSFS model, and their lower, upper, and calibrated values.

Processes	parameter	calibrated value	lower limit	upper limit
Snow and Precipitation correction				
	ZCPS	0.93	0.90	1.20
	CPL	0.99	0.90	1.10
Evaporation				
	CHP2	1.40	0.60	1.40
	ha_scal	1.02	0.95	1.05
Soil moisture and ground water model				
	EX	7.27	0.90	10.00
	EX2	0.90	0.90	10.00
	POM	0.80	0.80	1.20
	GC	0.10	0.00	0.10
	KR	1.00	0.10	1.00
	mv_dep1	9.00	9.00	15.00
	mv_dep2	30.00	30.00	90.00
	mv_rouA	0.98	0.00	1.00
	mv_rouM	1.00	0.00	1.00
	gv_EffPo	1.00	0.20	1.00
	gv_Drain	-0.20	-2.50	-0.20
Snow model (compaction)				
	sn_RI	0.91	0.91	0.93
	sn_QSMAX	0.07	0.03	0.09
	sn_C	0.01	0.00	0.05
Snow energy balance model				
	seb_DEN1	1.00	0.70	1.00
	seb_DEN2	0.71	0.70	0.90
	seb_HLIM	33.54	8.00	40.00
	seb_ALBM	0.85	0.70	0.90
	seb_CF1	0.83	0.75	1.00
	seb_CF2	0.11	0.07	0.22
	seb_CF3	0.33	0.10	0.50
	seb_DN	0.95	0.95	0.98
	seb_DNF	0.98	0.98	1.00
	seb_AUE	0.73	0.60	0.85
	seb_BUE	0.06	0.04	0.08
	seb_CL	0.11	0.10	0.14
	seb_CSEN	0.07	0.04	0.07
	seb_CSE1	0.23	0.15	0.23
	seb_CSE2	0.02	0.01	0.02
	seb_CLAT	1.22	0.70	1.50
	seb_WIND	0.60	0.10	0.60
	seb_CLTe	2.64	0.00	10.00

Table 2. The overland, porous media, and evapotranspiration related properties used for the Kälväsvaara HydroGeoSphere model acquired from Ala-aho et al., 2015 and Jaros et al., 2019). Leaf area index values were extracted from Härkönen et al. (2015), Räsänen et al. (2020), and Rautiainen et al. (2012).

Porous media properties	Esker sand	Glacial till	Peat acrotelm	Peat catotelm	Drained peat
Hydraulic conductivity					
Kx (m/s)	2.50E-05	2.15E-07	4.71E-04	2.15E-08	2.15E-08
Ky (m/s)	2.50E-05	2.15E-07	4.71E-04	2.15E-08	2.15E-08
Kz (m/s)	1.25E-06	1.08E-06	4.71E-07	2.15E-09	2.15E-09
Porosity φ (m^3/m^3)	0.4367	0.3267	0.8	0.8567	0.9267
Specific storage Ss (m^{-1})	0.0001	0.01	0.001	0.003684	0.003684
Unsaturated van Genuchten functions					
Residual saturation θr (m^3/m^3)	0.03	0.08	0.22	0.79	0.84
Alpha α (m^{-1})	1.1	1.4	25.17	5.033	30
Beta β (-)	1.4	2.1	1.1	1.2	2.283
Overland flow properties	Forest	Undisturbed peat	Drained peat	Channels	
Manning's n (s/[$m^{1/3}$])	0.6	0.01	0.4667	0.01	
Rill storage height (m)	0.15	0.5	0.01	0.01	
Obstruction storage height (m)	0.3	0.07333	0.01	0.01	
Coupling length (m)	0.001	0.01	0.0001	0.1	
Evapotranspiration properties	Forest	Peat			
Canopy storage parameter (m)	0	0			
Initial interception storage (m)	0	0			
Transpiration fitting parameters					
C1 (-)	0.4	0			
C2 (-)	-0.1	0.5			
C3 (-)	1	1			
Transpiration limiting saturations					
Saturation at wilting point (-)	0.06	0.06			
Saturation at field capacity (-)	0.25	0.15			
Saturation at oxic limit (-)	0.6	0.99			
Saturation at anoxic limit (-)	0.9	1			
Evaporation limiting saturations					
Saturation below which evaporation is zero (-)	0.04	0.1			
Saturation above which full evaporation can occur (-)	0.37	0.25			
Leaf area index of entire model (-)	1.80	0.88			
Maximum root depth (m)	1	1			
Root length density function	Quadratic decay function	Quadratic decay function			
Maximum evaporation depth (m)	1	1			
Evaporation function	Quadratic decay function	Quadratic decay function			
Snowmelt constants					
Snow density (kg/m^3)	1000				
Melting constant ($kg*m^{-2}*T^{-1}*[1/°C]$)	9.8379E-6				
Sublimation constant ($kg*m^{-2}*T^{-1}$)	0.0				
Threshold temperature (°C)	0.0				
Initial snow depth 1.1.2015 (m)	0.01228				

4 Results

4.1 WSFS and HGS models calibration and validation performances

4.1.1 WSFS model performance

WSFS and HGS models were both simulated between years 2015 and 2020. The WSFS hydrologic model of the watershed was calibrated between years 2015 and 2020 at four discharge observation points (Figure 3a) and validated using the data obtained between 2021 and 2022. The steady state HGS model uses calibrated parameter set for subsurface and overland properties following the values by Jaros et al. (2019). Transient, three dimensional HGS model was not calibrated due to lack of sufficient monitoring data from the time of interest (2015-2020) and model's long computing times. The discharge observation monitoring points used in WSFS model calibration and validation couldn't be used for the HGS model since they were outside of its domain perimeter.

The WSFS model was able to produce a very good fit between simulated and observed discharges despite its short calibration and validation periods. During the calibration stages of the WSFS model, Nash-Sutcliff efficiency values for discharge stations i6000100q, i6000110q, i6000200q, and i6000410q were 0.78, 0.66, 0.76, and 0.75, respectively, while the Nash-Sutcliff efficiency values during the validation stages were 0.42, 0.65, 0.65, and 0.03 (Figure 6, Figure 7, Figure 8, Figure 9).

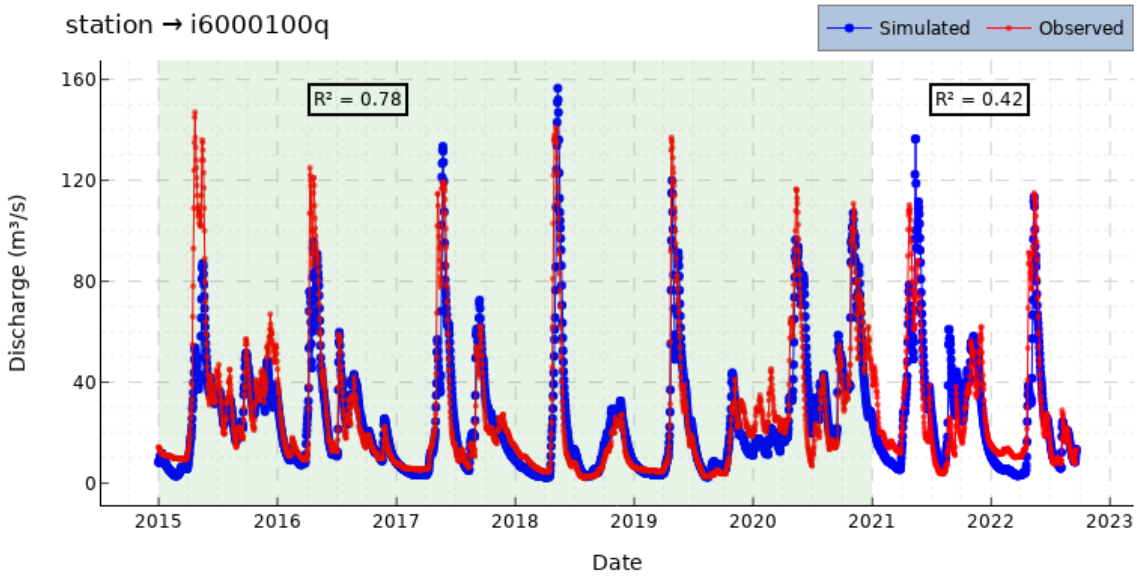

Figure 6. At the i6000100q station, the WSFS model calibration (green shaded region, 2015 to 2020) and validation (2021 to 2022) stages are shown, as well as their corresponding Nash-Sutcliff efficiency (R^2) values.

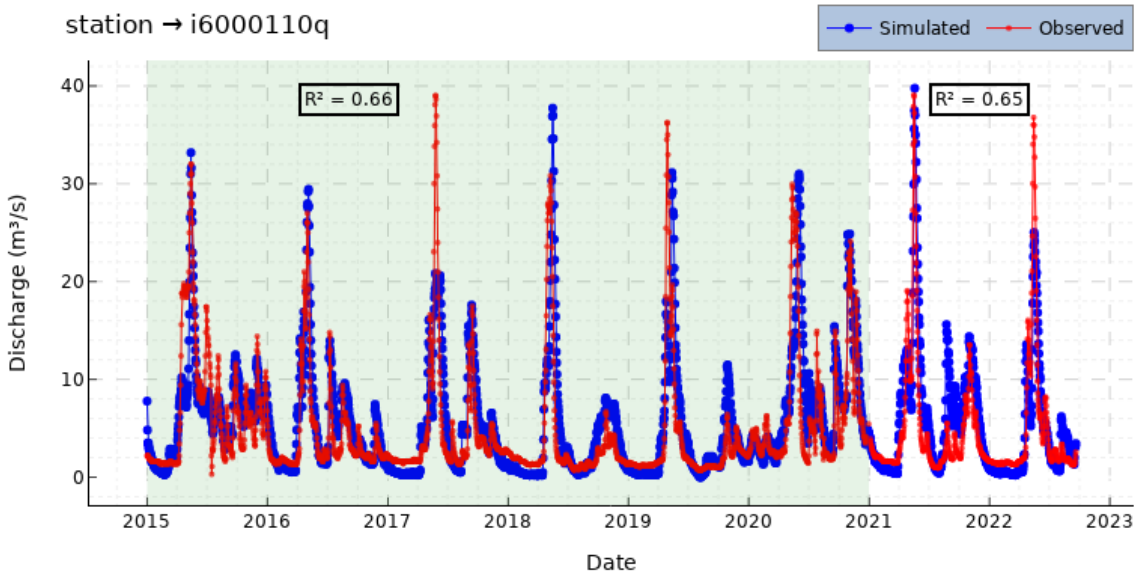

Figure 7. At the i6000110q station, the WSFS model calibration (green shaded region, 2015 to 2020) and validation (2021 to 2022) stages are shown, as well as their corresponding Nash-Sutcliff efficiency (R^2) values.

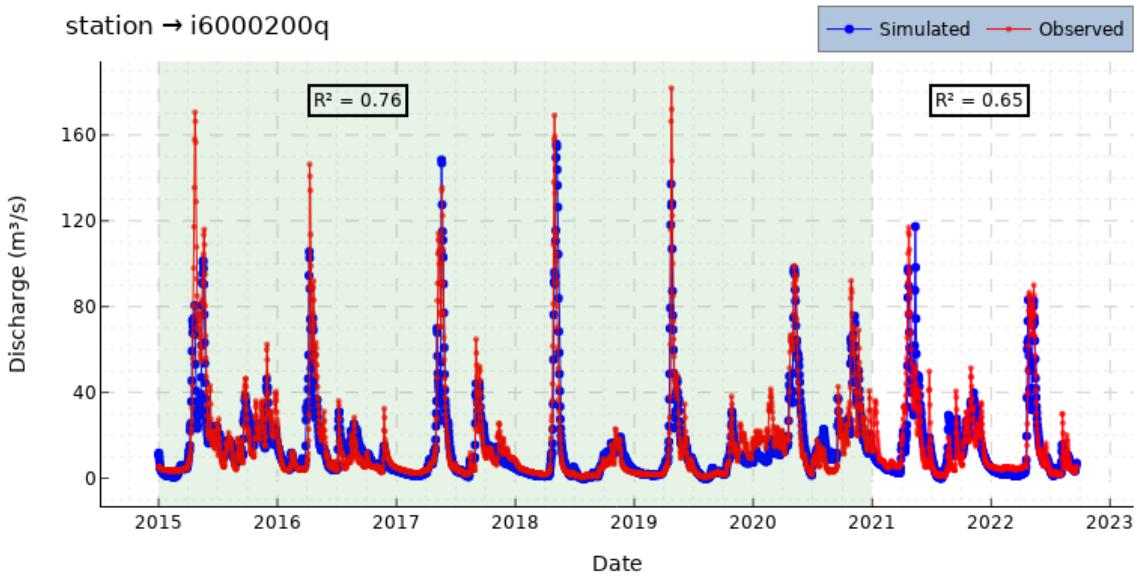

Figure 8. At the i6000200q station, the WSFS model calibration (green shaded region, 2015 to 2020) and validation (2021 to 2022) stages are shown, as well as their corresponding Nash-Sutcliff efficiency (R^2) values.

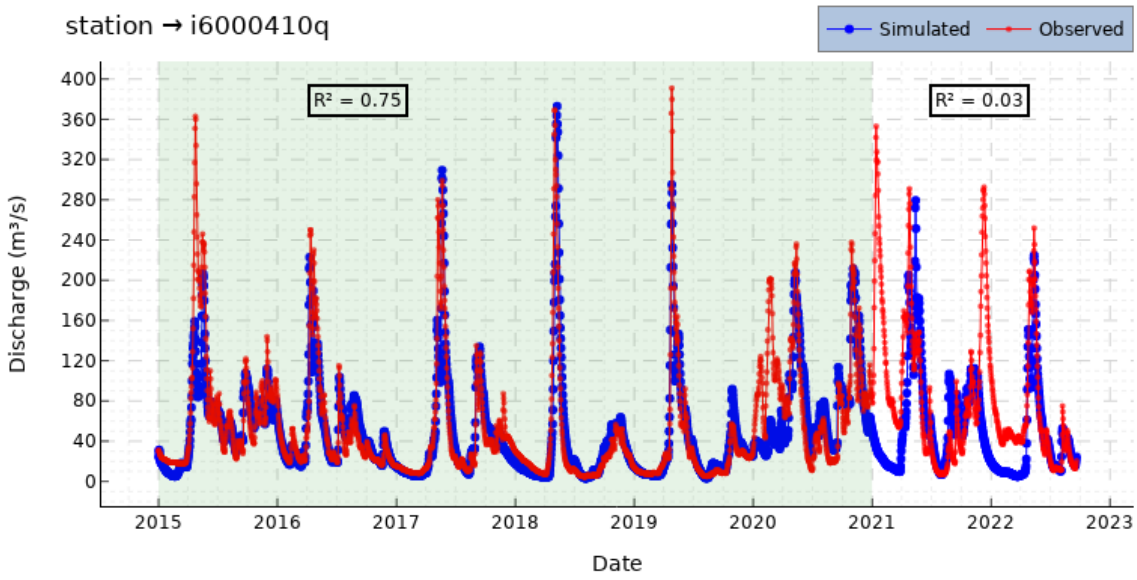

Figure 9. At the i6000410q station, the WSFS model calibration (green shaded region, 2015 to 2020) and validation (2021 to 2022) stages are shown, as well as their corresponding Nash-Sutcliff efficiency (R^2) values.

4.1.2 HGS model performance

The HGS model performance was evaluated by comparing simulated and observed water levels at three lakes and 29 groundwater monitoring wells (87 measurements) in the simulation period (2015-2020) (Figure 10). A few groundwater monitoring sites showed satisfactory groundwater levels when observed data was compared to simulated data. Despite this, groundwater levels were significantly different between measured and simulated by up to eight meters (Figure 10, b). Average absolute error of the groundwater well measurements and modelled water tables was 2.72 m, and the root mean squared error RMSE was 3.61. The long-term simulated average water levels for the first two lakes/ponds showed reasonable agreement with observations (differ by 0.12 m, and 0.74 m), but the third lake was off by about 10 meters (Figure 10, c). Possibly, this significant difference is due to Pieni Kirkaslampi (Figure 10 c) being located on a perched aquifer that the HGS model did not account for.

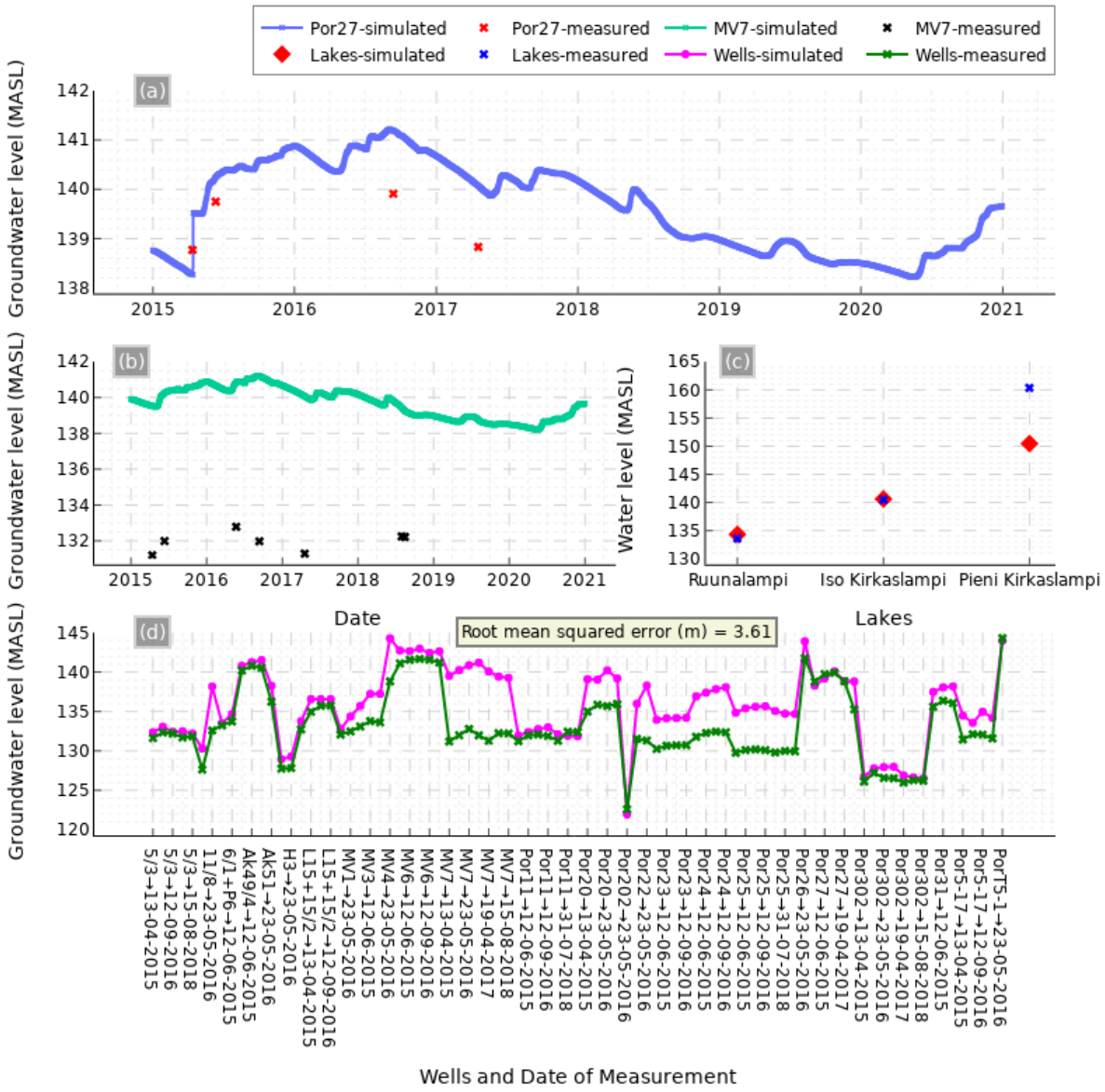

Figure 10. The HGS model simulations and performance (a) observed and simulated groundwater levels at well Por27, (b) observed and simulated groundwater levels at well MV7, (c) observed and simulated (long-term average) water levels at three lakes, and (d) observed and simulated groundwater levels at all wells, and the root mean squared error.

Furthermore, in the peatland area, daily simulated and observed water levels at 11 locations within the peat layer were compared. Some of the peatland points were in Olvassuo area north of the Kälväsvaara aquifer, and some in the proximity of the Kälväsvaara aquifers southern border. In the peatland area, the model overestimated water table in all the measuring points (the peatland area was flooded for almost the whole modelling period). Unexpected errors were also observed in the modelled water table depth values (sudden changes and unrealistic

negative values) which have been discussed with the HGS model developers. Peatland areas around some of the peatland observation points were restored during the modelling period. This restoration wasn't considered which added more uncertainty into the model. Drainage was considered via parameters.

4.2 WSFS and HGS results comparison

We compared the WSFS-simulated soil moisture (volumetric moisture content in m3/m3) for a variety of soil types in the two soil layers above the i6000200q discharge calibration station (closest station to the HGS model area) with the HGS-simulated average soil moisture for each soil layer in the shaded area. Furthermore, a comparison of soil moisture averages in each third level subbasin and shaded area (HGS model area, Figure 3) was also made between WSFS and HGS, respectively. We compared shallow groundwater storage changes simulated by WSFS in third level subbasins 60.043 (60_gv60_043), 60.066 (60_gv60_066), and 60.075 (60_gv60_075) with those simulated by HGS in the shaded region (Figure 3). A comparison was made between WSFS-simulated evapotranspiration of various soil types above the i6000200q discharge calibration station (closest station to the HGS model area) and HGS-simulated evapotranspiration of various soil types in the shaded area. Furthermore, comparisons between the average evapotranspiration simulated in WSFS and HGS, respectively, were made in each third level subbasin and shaded area (HGS model area, Figure 3).

4.2.1 Soil moisture in the top and bottom layers

The modelling area has a high proportion of organic soils, which can cause rapid soil moisture response in the upper layer due to their high hydraulic conductivity, as well as other factors, such as evapotranspiration, which is reflected in the WSFS simulations, and verified by observed SMOS soil moisture data, but not by HGS simulations, suggesting possible errors in the HGS model representation (Figure 11, Figure 13). In spring, summer, and autumn, WSFS simulations showed frequent and large fluctuations in soil moisture, whereas HGS simulations fluctuations were similar in timing especially for the years 2017-2020 but didn't share the magnitude. Moreover, as shown in Figure 11 and Figure 13, observed remote sensing soil moisture data from SMOS satellite was more consistent with WSFS simulated soil moisture than HGS.

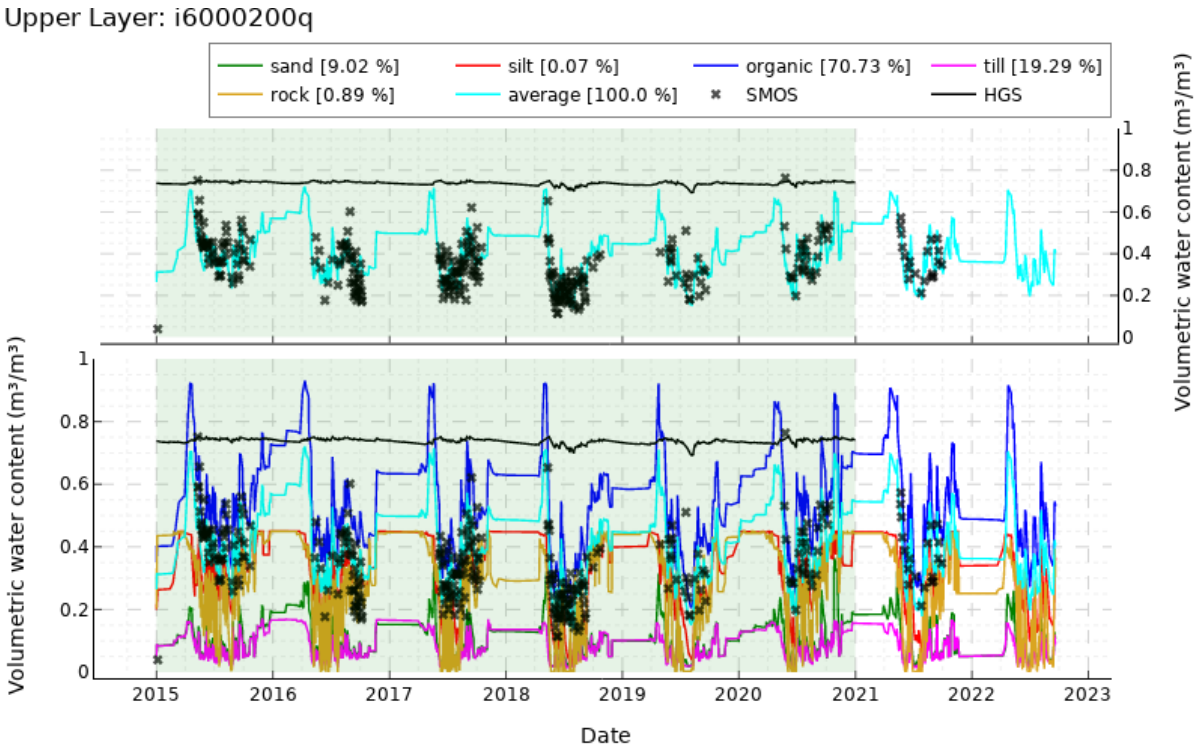

Figure 11. A comparison of the top layer soil moisture simulated by WSFS (for the area above i6000200q station) for each soil type (soil percentage coverage shown in the legend) and HGS (HGS model area) to the observed remote sensing soil moisture data by the SMOS satellite. The top figure compares the average soil moisture simulation of WSFS with HGS and observed SMOS data.

The WSFS simulations of soil moisture in the bottom layer had lower values and gentle fluctuations due to lower hydraulic conductivity and higher bulk density than in the upper layer, whereas HGS simulations showed unrealistically large values with minimal fluctuations (Figure 12, Figure 14). The HGS simulated soil moisture in both lower and upper layers differed significantly from WSFS, and the HGS simulated soil moisture differed significantly and was not comparable with SMOS observations (Figure 11, Figure 13, Figure 13, Figure 14).

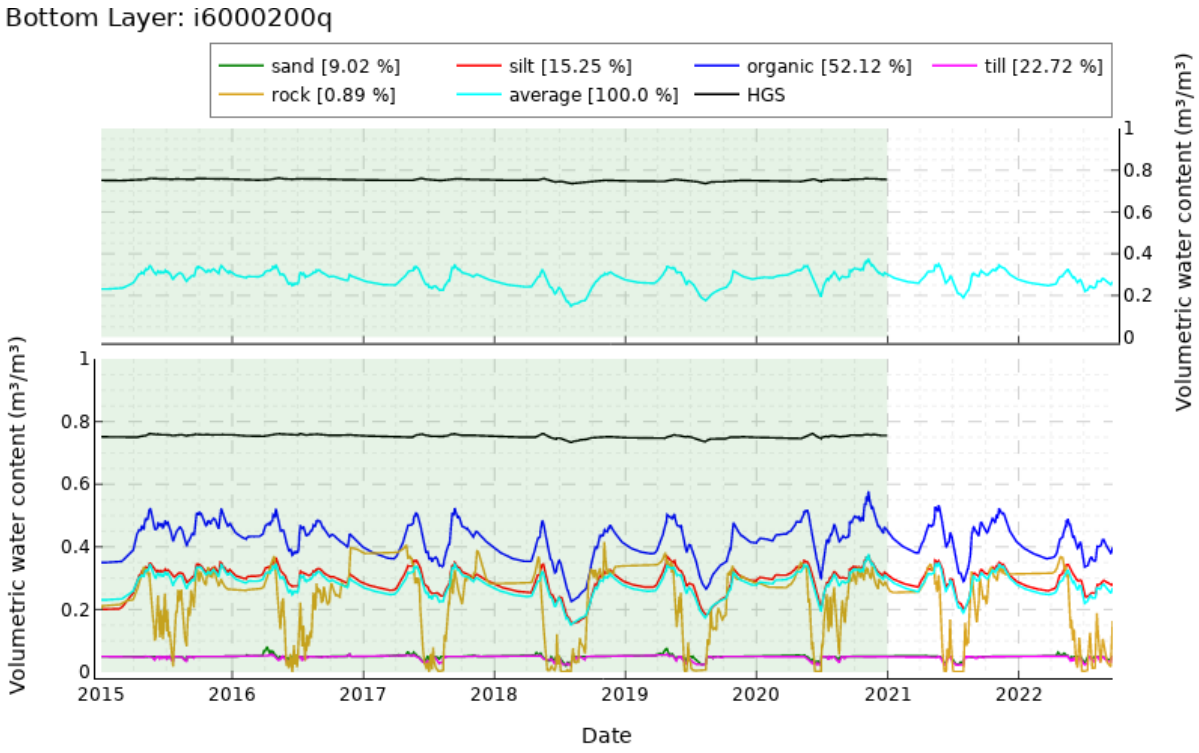

Figure 12. A comparison of the bottom layer soil moisture simulated by WSFS (for the area above i6000200q station) and HGS (for HGS model area). The top figure compares the average soil moisture simulation of WSFS and HGS for the respective model areas.

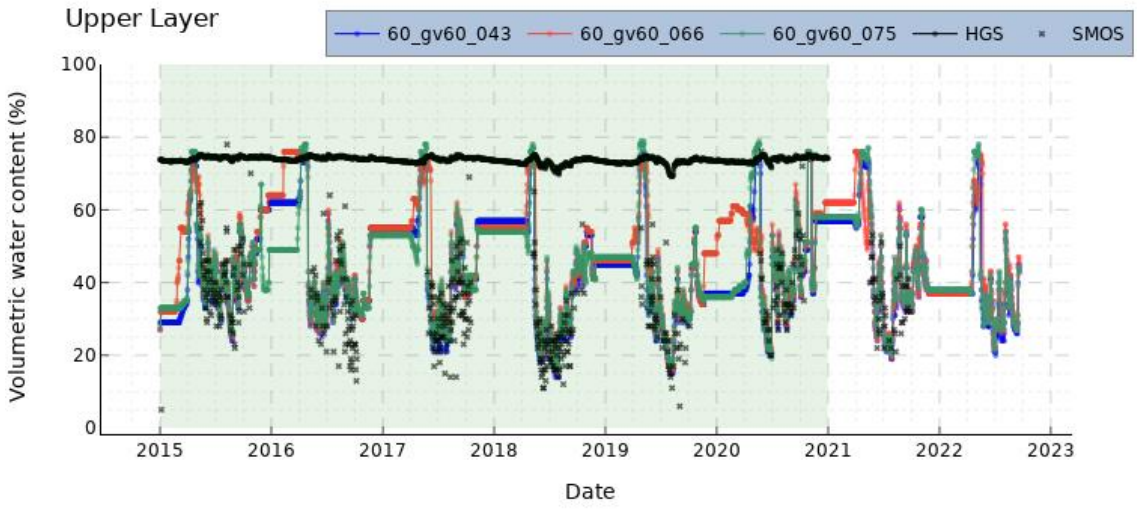

Figure 13. A comparison of average soil moisture of the top layer simulated using WSFS (for the three subbasins near the HGS model area) and HGS (HGS model area) to the observed remote sensing soil moisture data by the SMOS satellite.

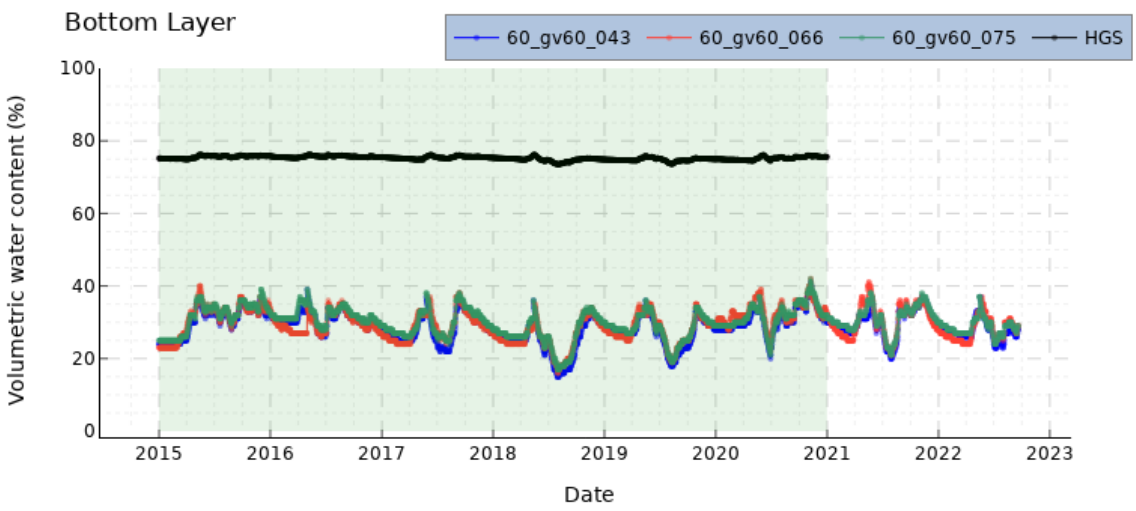

Figure 14. A comparison of average soil moisture of the bottom layer simulated by WSFS (for three subbasins near the HGS model area) and HGS (HGS model area).

Statistical comparisons between HGS and WSFS soil moisture on a weekly, monthly, seasonal, and yearly basis (Figure 15 to Figure 22) proved that HGS soil moisture did not differ much even though the precipitation and temperature changed greatly during those periods. An analysis of the HGS simulated soil moisture of the upper layer on a yearly, seasonal, monthly, and weekly basis showed that there were no significant differences, with an average soil moisture value ranging from 0.73 to 0.74, with a standard deviation (STD) of 0.01 (Figure 15 to Figure 18). As confirmed by observed SMOS soil moisture data, the WSFS model soil moisture simulations in the upper layer were more realistic and showed significant differences between weeks, months, seasons, and years. The WSFS simulated upper layer soil moisture varied on average between 0.38 and 0.50 and STD between 0.11 and 0.12, respectively. The WSFS model indicated that the average seasonal soil moisture ranged between 0.32 and 0.57, while the corresponding STD varied between 0.09 and 0.13, and the rest can be seen in Figure 15 to Figure 18. In Figure 16 of the WSFS simulated upper layer soil moisture for the years 2015 to 2022, June and July were the months with the lowest soil moisture, and April and May had the highest soil moisture. Furthermore, Figure 19 to Figure 22 compare statistically the simulations of soil moisture in the bottom layer of both models.

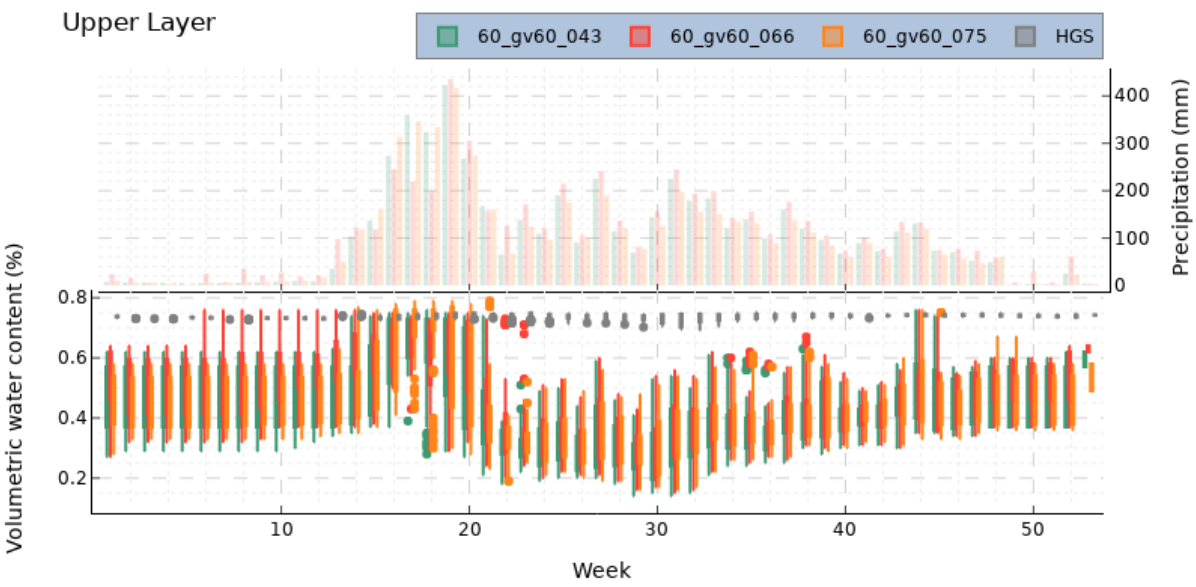

Figure 15. A weekly statistical comparison of WSFS and HGS simulated soil moisture in the upper layer for the years 2015 to 2020.

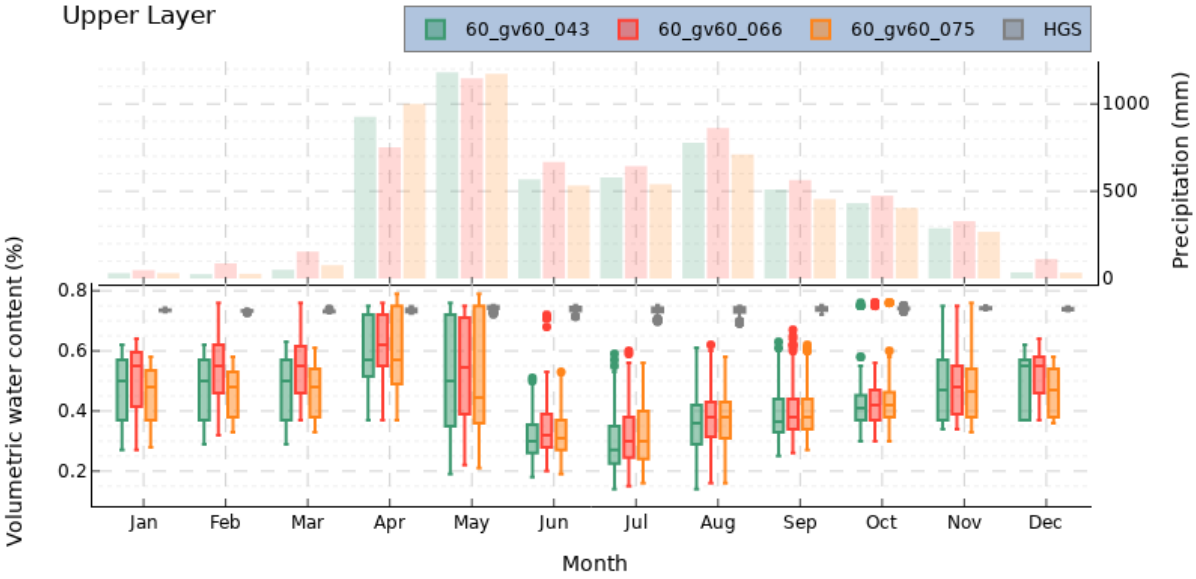

Figure 16. A monthly statistical comparison of WSFS and HGS simulated soil moisture in the upper layer for the years 2015 to 2020.

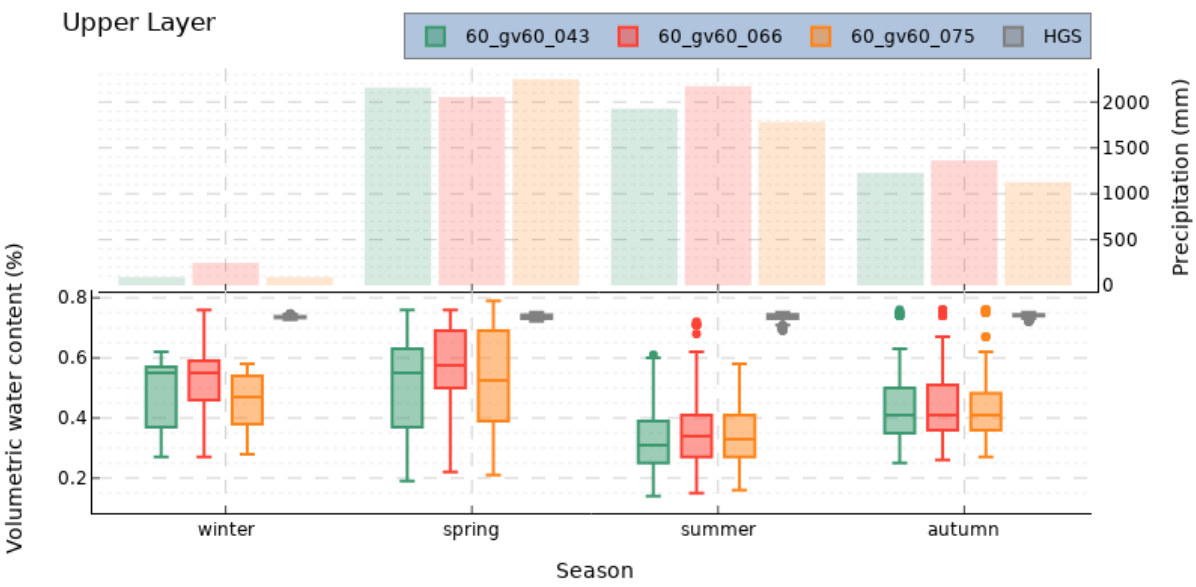

Figure 17. A seasonal statistical comparison of WSFS and HGS simulated soil moisture in the upper layer for the years 2015 to 2020.

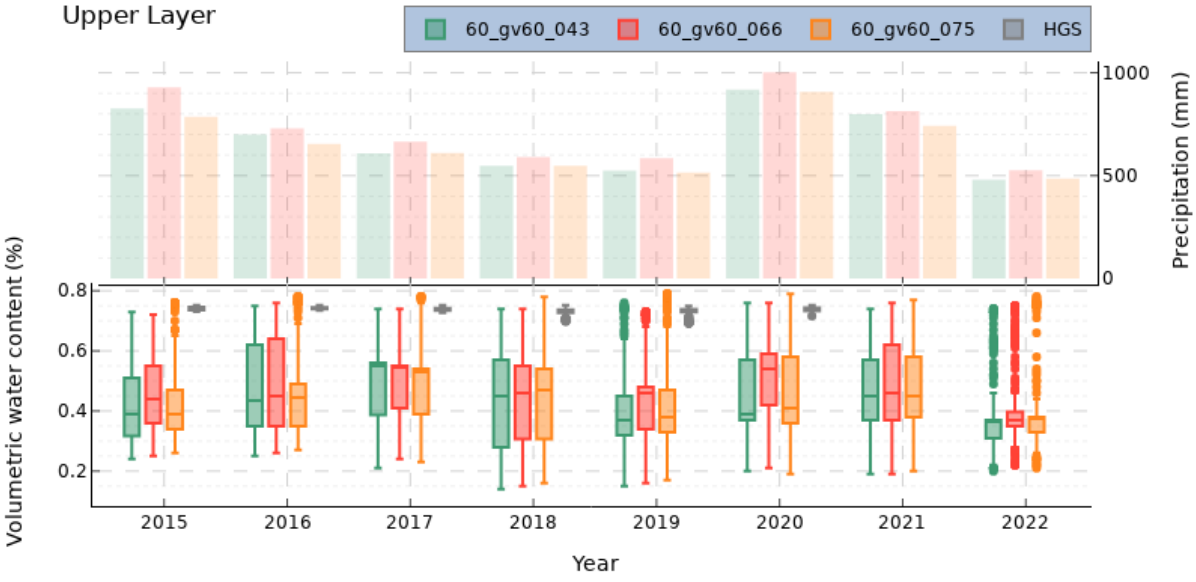

Figure 18. A yearly statistical comparison of WSFS and HGS simulated soil moisture in the upper layer for the years 2015 to 2020.

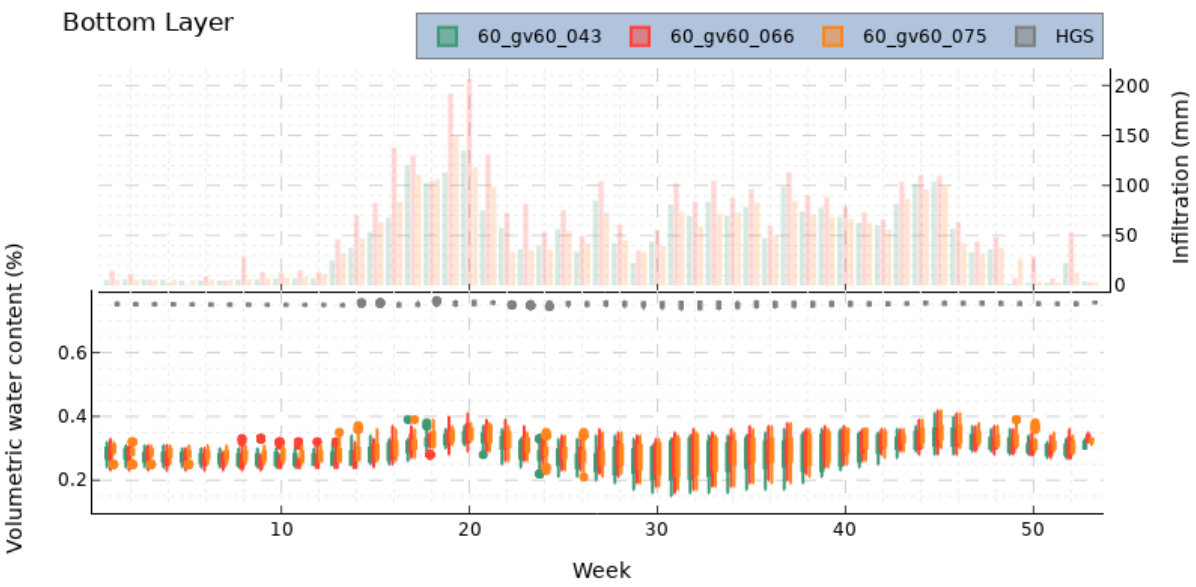

Figure 19. A weekly statistical comparison of WSFS and HGS simulated soil moisture in the bottom layer for the years 2015 to 2020.

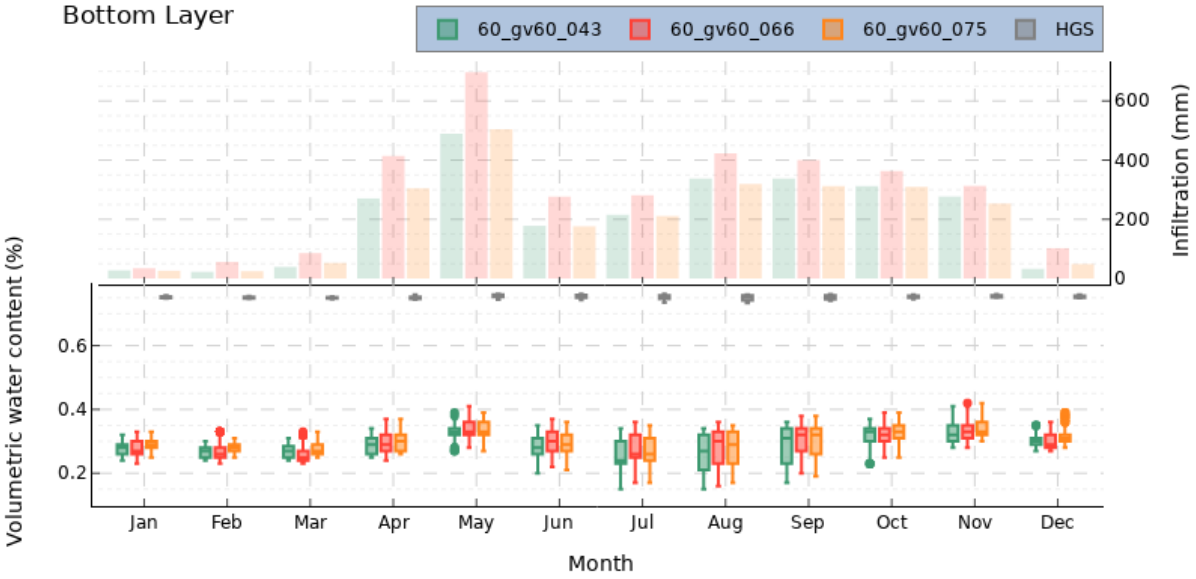

Figure 20. A monthly statistical comparison of WSFS and HGS simulated soil moisture in the bottom layer for the years 2015 to 2020.

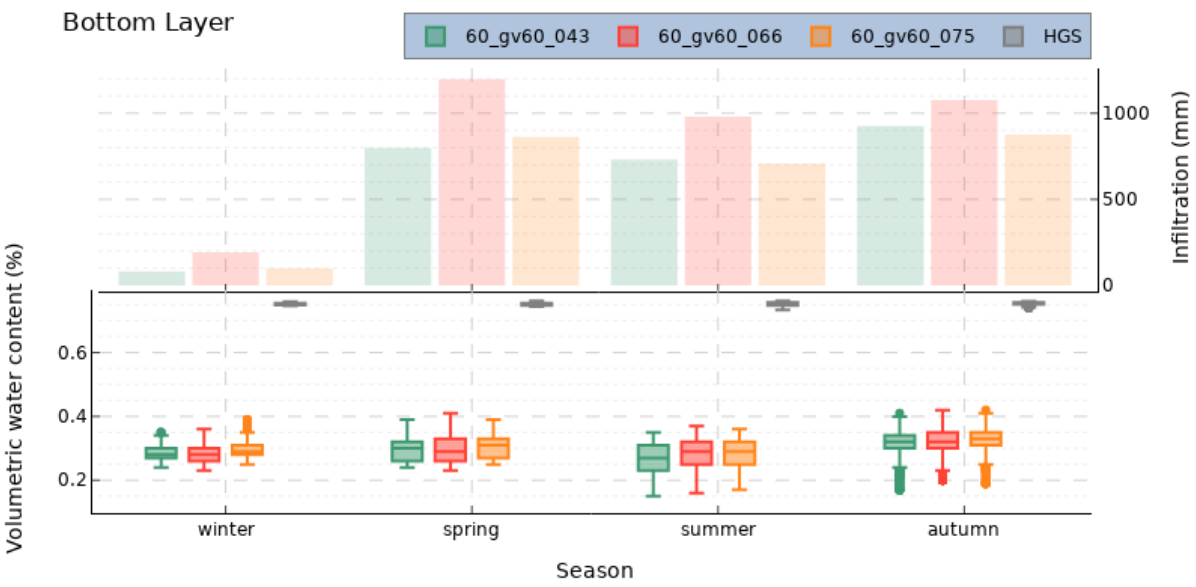

Figure 21. A seasonal statistical comparison of WSFS and HGS simulated soil moisture in the bottom layer for the years 2015 to 2020.

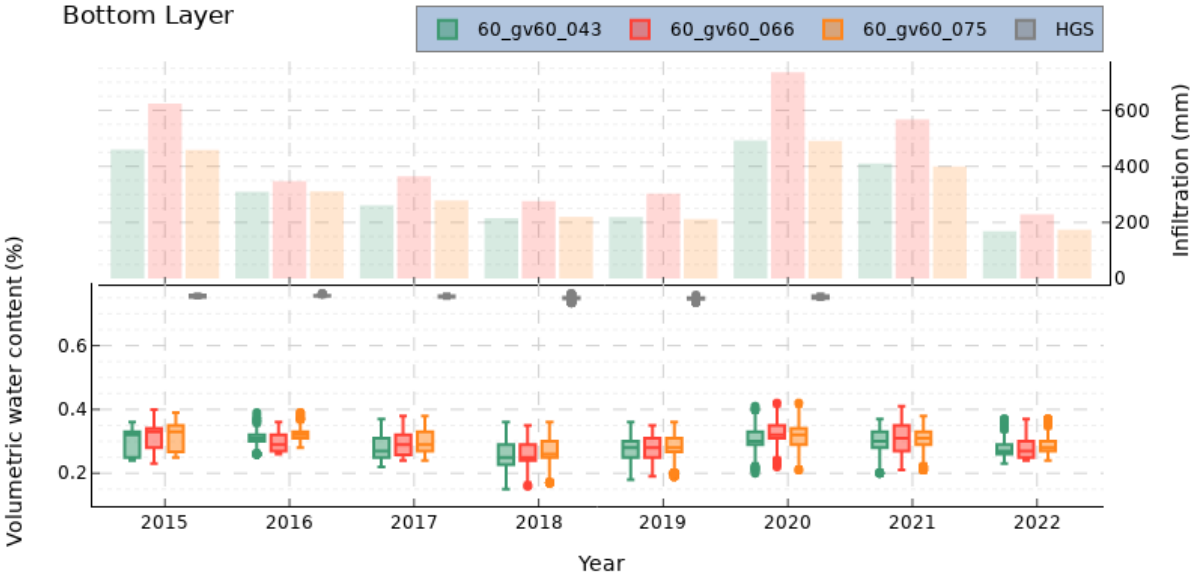

Figure 22. A yearly statistical comparison of WSFS and HGS simulated soil moisture in the bottom layer for the years 2015 to 2020.

4.2.2 Shallow groundwater storage

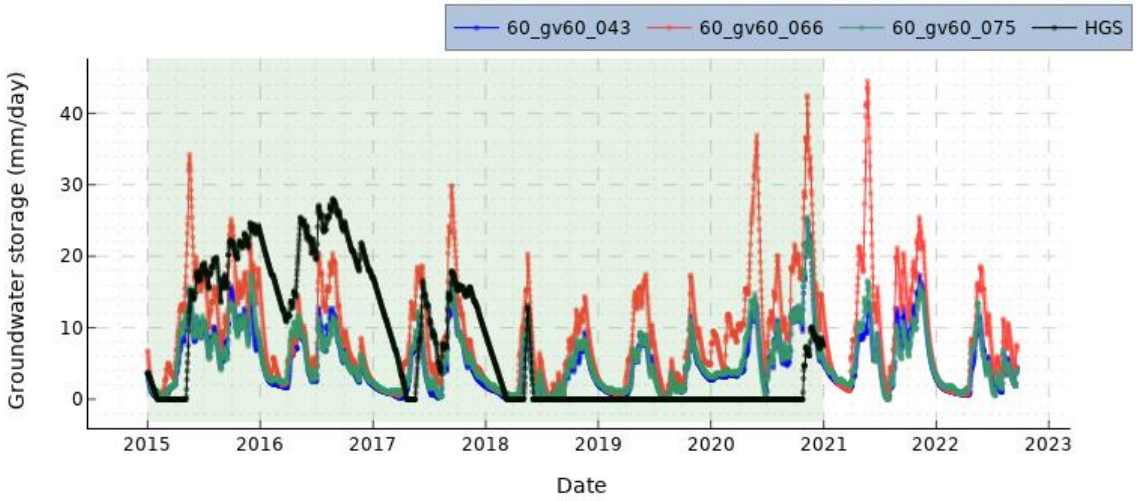

Figure 23. A simulation of the groundwater storage gain for the WSFS and HGS models for each subbasin, and HGS model area, respectively.

WSFS simulated groundwater storage gain showed high fluctuation and the subbasins seemed to respond in a similar pattern, with 60_gv60_066 having the highest peaks (Figure 23). Compared to soil moisture, HGS simulated groundwater storage gain corresponded somewhat better with WSFS for the early simulation years. HGS output included some of the fluctuation, but overall WSFS storage gain fluctuation was higher and response sharper. For the late simulation years from mid-2018 onwards, the HGS results did not match well with the WSFS results (Figure 23). Yearly statistical comparison of the simulated groundwater storage gain shows significant difference in WSFS and HGS simulated values (Figure 27). Seasonal fluctuation in the WSFS simulated values were higher and, spring and autumn recharge periods were more clearly visible, but late winter dry period was visible in the HGS results also (Figure 24 to Figure 27).

Figure 24. A weekly statistical comparison of WSFS and HGS simulated shallow groundwater storage for the years 2015 to 2020 for each subbasin and HGS model area, respectively. The percolation is from WSFS model.

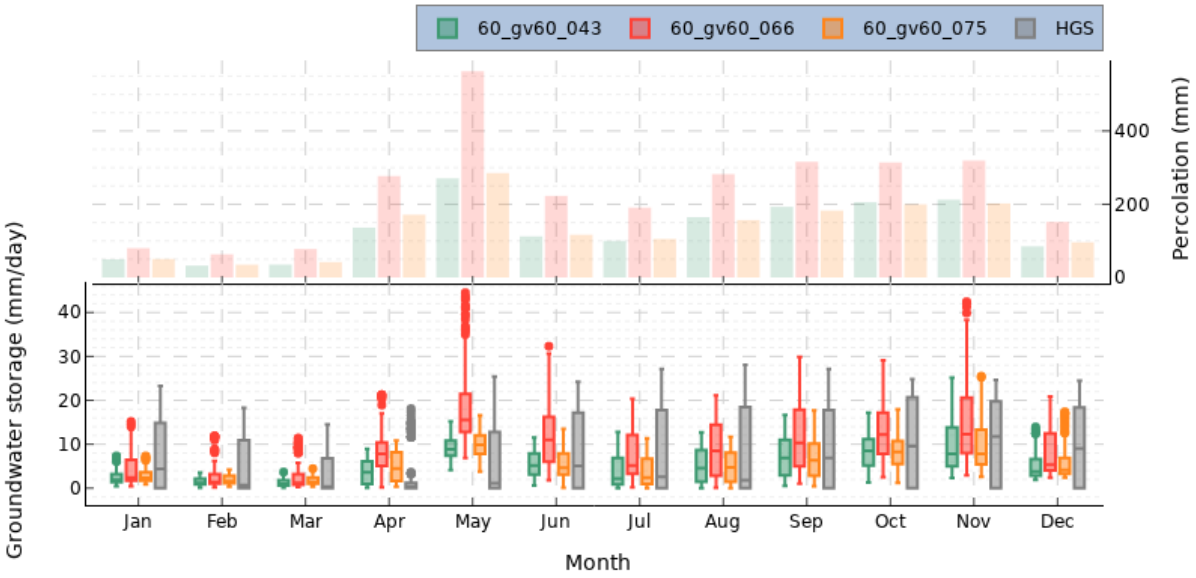

Figure 25. A monthly statistical comparison of WSFS and HGS simulated shallow groundwater storage for the years 2015 to 2020 for each subbasin and HGS model area, respectively. The percolation is from WSFS model.

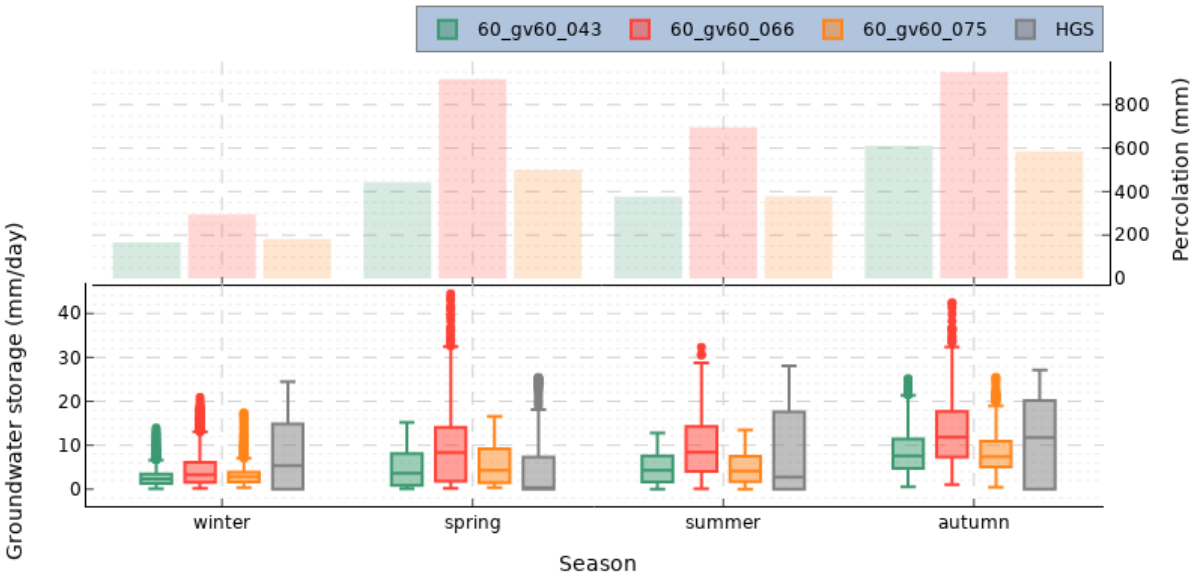

Figure 26. A seasonal statistical comparison of WSFS and HGS simulated shallow groundwater storage for the years 2015 to 2020 for each subbasin and HGS model area, respectively. The percolation is from WSFS model.

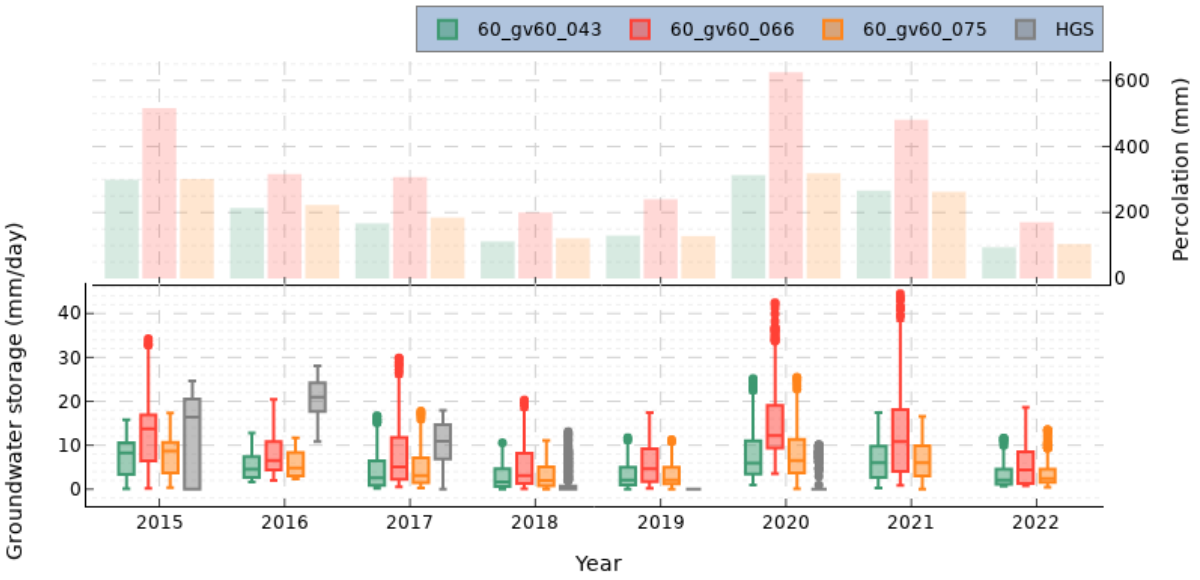

Figure 27. A yearly statistical comparison of WSFS and HGS simulated shallow groundwater storage for the years 2015 to 2020 for each subbasin and HGS model area, respectively. The percolation is from WSFS model.

4.2.3 Evapotranspiration

Simulated actual evapotranspiration of both HGS and WSFS models were compared statistically in Figure 28 to Figure 32. The WSFS and HGS evapotranspiration values followed

a similar pattern: during the summer, for example, high temperatures and leaf canopy create favorable evapotranspiration conditions, whereas during the winter, the cold temperatures, snow cover and frozen ground resulted in close to zero evapotranspiration. The HGS simulations simulated higher evapotranspiration in the hot summers of 2018 and 2019, but overall, the HGS simulations simulated significantly lower evapotranspiration than the WSFS simulations (Figure 28 to Figure 32). The WSFS simulated evapotranspiration values in 2015 and 2016 were significantly greater than HGS simulated values, but in 2017-2020 they were more closely correlated, and in the year 2018 they were received closest correlation (Figure 28 to Figure 32).

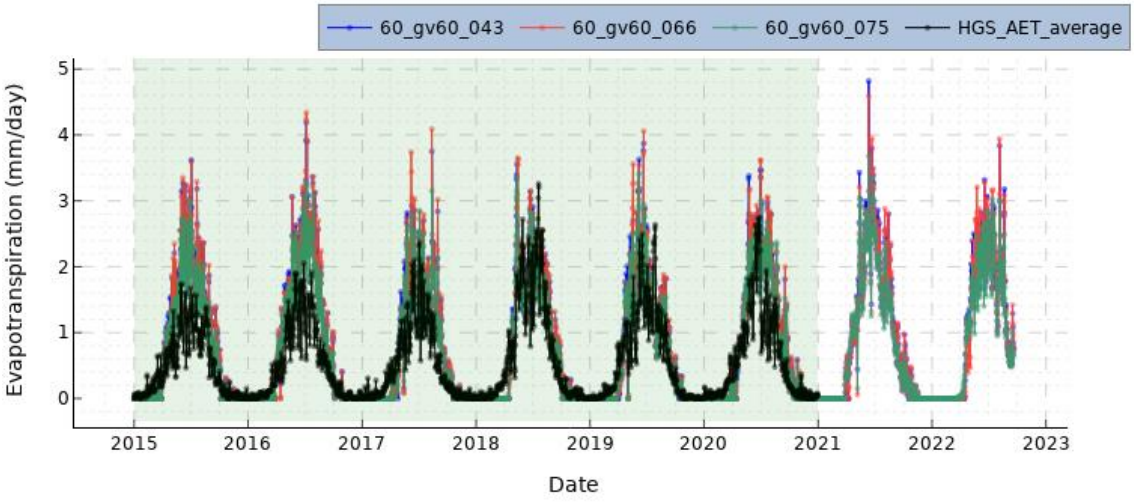

Figure 28. The WSFS and HGS model evapotranspiration simulations for each subbasin and HGS model area, respectively.

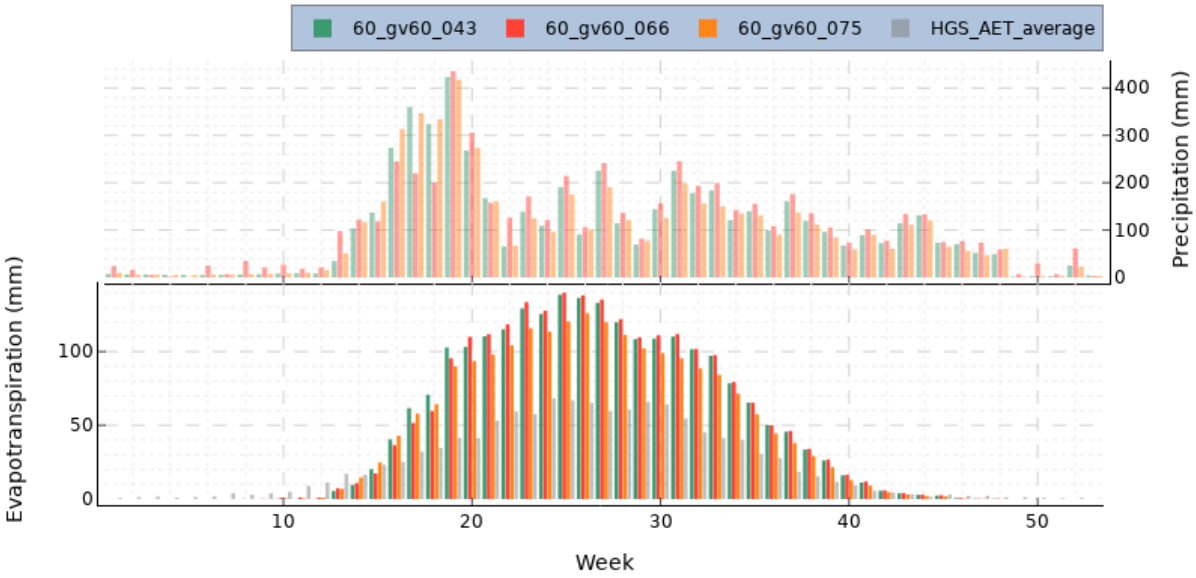

Figure 29. A weekly statistical comparison of WSFS and HGS simulated evapotranspiration from 2015 to 2020.

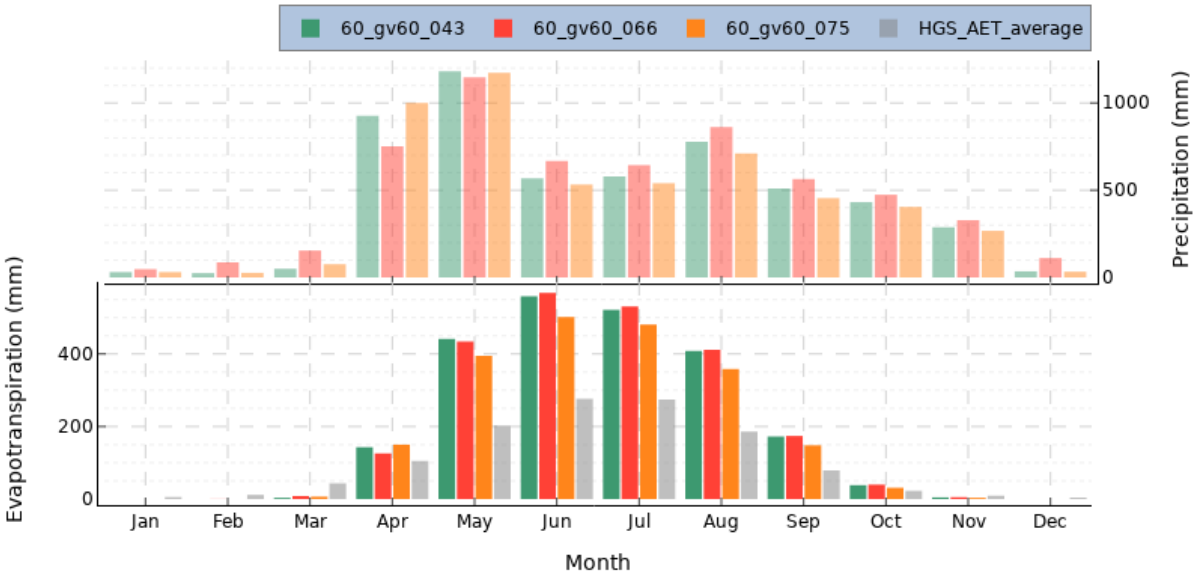

Figure 30. A monthly statistical comparison of WSFS and HGS simulated evapotranspiration from 2015 to 2020.

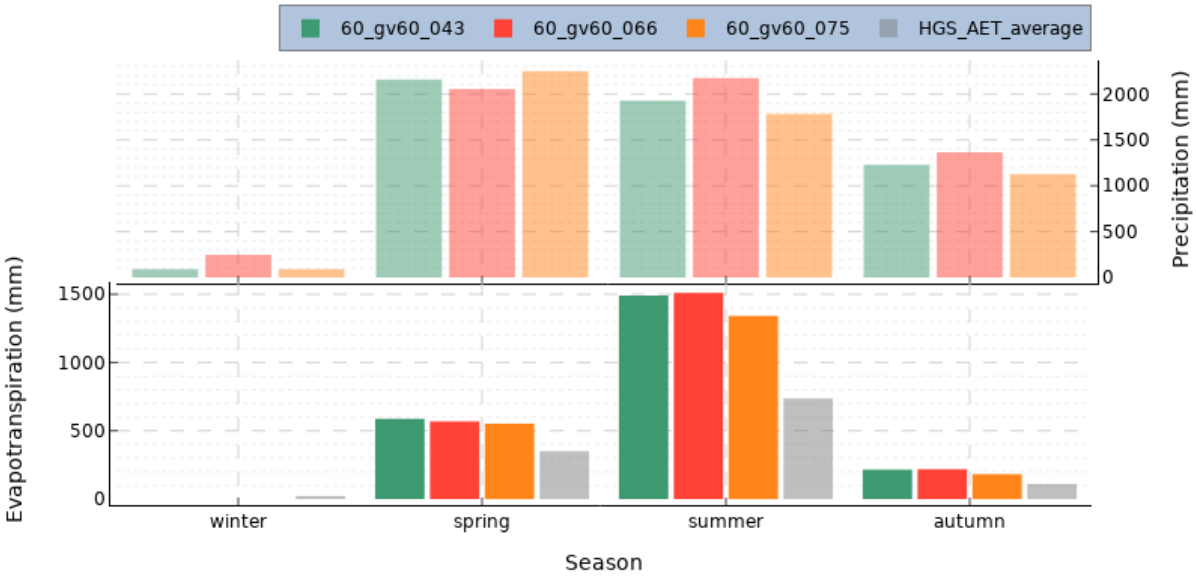

Figure 31. A seasonal statistical comparison of WSFS and HGS simulated evapotranspiration from 2015 to 2020.

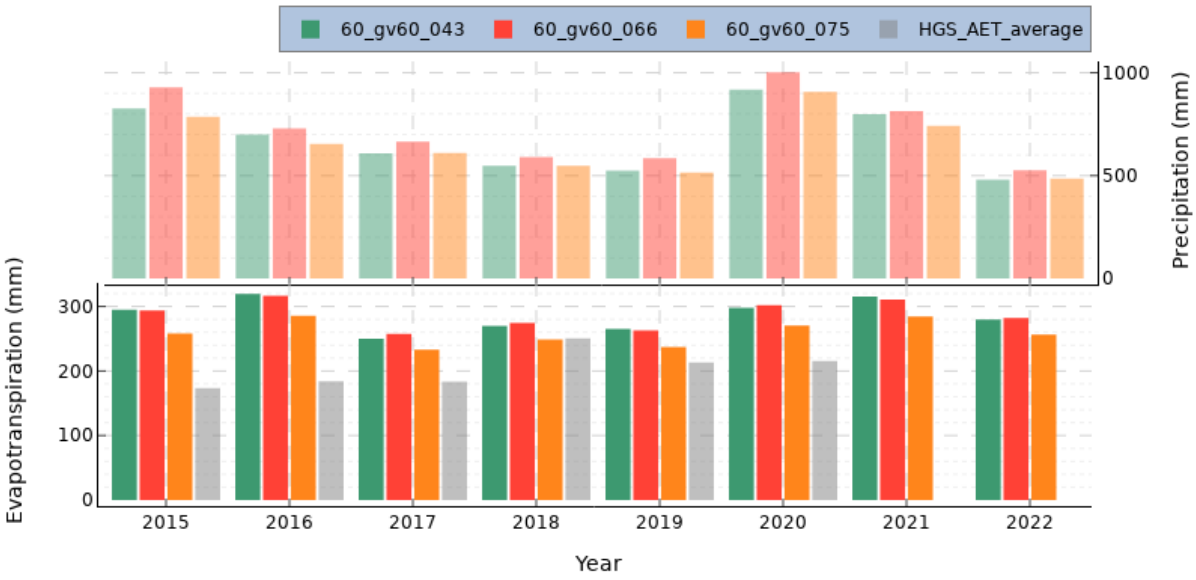

Figure 32. A yearly statistical comparison of WSFS and HGS simulated evapotranspiration from 2015 to 2020.

5 Discussions

5.1 The strengths and weaknesses of the two hydrologic models (HGS and WSFS)

5.1.1 The HGS hydrologic model

The main strength of a fully integrated HGS model is its ability to accurately represent surface and groundwater flows, allowing precipitation to partition into all key hydrologic components in a natural, physically-based manner (Brunner & Simmons, 2012). Fully integrated models like the HGS can simulate feedback between surface and subsurface domains and solve complex problems in a more realistic way than simple semi-distributed models. HGS can, for example provide output of the vertical and horizontal fluxes of different, defined soil layers. However, the HGS three-dimensional model requires a lot of input data (e.g., topography, soil, land use, and climatic data); some of which are difficult to obtain.

A previous study by Jaros et al. (2019) investigated parameter sensitivity of a steady-state HGS model of the Kälväsvaara esker aquifer and its surrounding peatlands, and identified the most influential parameters. Still, when uncertain and random parameters are used in the van-Genuchten functions, the results can be physically irrelevant but nonetheless have a significant impact on results obtained by the HGS model. It is therefore necessary to carefully select the parameters via measurements, calibration runs, or with previous studies. Hence, in our HGS model, we used the parameters that Jaros et al. (2019) suggested to be the best for their steady state model. Evapotranspiration properties were obtained from literature, and they should be better parametrized because of the underestimation of the evapotranspiration values compared to WSFS model. Underestimation in evapotranspiration can also have a significant effect on overall HGS model heads and soil moisture values.

In our HGS model, the geomorphological data were not accurately represented due to oversimplification of the complex system. Modelled Aapa mire complexes vary significantly in peat depth from a few centimeters in the margin regions to several meters in the wet central regions (R. Heikkilä et al., 2006). However, in the HGS model, we used the average peat depth to represent the peat layer. Most of the groundwater interactions between peat and the soil underneath occur in areas of sudden depth change in the peat layer (R. Heikkilä et al., 2006), which are poorly represented in our HGS model due to uniform peat layer thickness. We assigned uniform porous media properties to the aquifer due to difficulties in accurately representing the soil complexity of Kälväsvaara esker, contributing to model errors. For

transient state modelling, we used only the years 2015 to 2020 due to the lack of measured input data. Only measured water table data was available. However, to improve model accuracy, more and different measured data would be required, which would then be divided into spin-up, calibration and validation period runs.

Additionally, the HGS model requires a great deal of computing power to run, making calibration and validation steps time consuming. When model runs are extended, output files can grow so that they are hard to handle with general computers. This problem has though been recognized by the software developer, and for example the newest version of HGS has an option of binary output instead of ASCII. Fully integrated modelling with HGS requires many pre- and post-processing steps that require strong computer skills from the user.

5.1.2 The WSFS hydrologic model

Like the HGS model, the Finnish Environment Institute's semi-distributed conceptual hydrologic model, the WSFS model, has its own strengths and weaknesses. Although the model is less complex, WSFS has many input parameters that represent watershed properties and hydrological processes. Many of these WSFS parameters cannot be measured directly for various reasons: (a) some of the parameters are difficult to measure directly, (b) some parameters have no physical meaning because they are derived from empirical estimations and literature references, (c) some of the parameters have high spatial variability (e.g., hydraulic conductivity of organic soils), and (d) the model has many parameters that need calibration, which might lead to equifinality, which occurs when multiple parameter sets provide equally acceptable results, making it difficult to choose one parameter set. Additionally, one third of Finland's land area is covered with mires and peat and the hydrological processes in these wet organic soil areas are poorly defined in the WSFS model, thus requiring further improvement. Another weakness of the WSFS model is that it does not consider deep groundwater flow between sub-basins, water flow between grid-cells within subbasins and other possible hydrological interactions, such as between wetlands and minerals soils. In the current version of WSFS, there are still key functionalities that do not exist, such as sensitivity analysis and the division of calibration period into calibration and validation period, which is currently under discussion for implementation.

Both the WSFS and HGS models require a large amount of input parameters. However, calibrating and estimating parameters of a fully integrated HGS model can be very challenging

because of the large number of parameters required and the long running times of the model. As compared to the HGS model, the WSFS has several advantages, including the ability to simulate large-scale watersheds relatively faster, making it possible to study climate change scenarios, land use changes, and management changes more efficiently, as well as forecast floods with much ease. The HGS model can be applied to the above-mentioned cases, but it requires a lot of computing power, more input data, which is always hard to obtain, and a long simulation period. Still, HGS can provide high spatial and temporal resolution outputs such as saturation maps, groundwater levels, heads, exchange rates between overland and porous media domain etc. Some potential possible outputs of HGS are represented in Figure 33. In ideal conditions, such as in the absence of time and resource constraints, a fully integrated HGS model that partitions input precipitation data into all key components of the hydrologic cycle, produces a more realistic result than the semi-distributed conceptual WSFS model. This could be used to understand changes in groundwater flow due to e.g., land use changes and the effects to groundwater dependent ecosystems.

WSFS and HGS model domains were different in our case: WSFS combined three third-level subbasins where HGS modelled an aquifer with the surrounding peatlands, which do not represent a single basin. The resolution of the data is somewhat different in the cases, which makes comparing the results difficult. HGS model domain was selected because of the good data and previous studies on the area, but to better compare the two very different models the modelled areas should be same. HGS model domain consists mostly of peat soils, and on a large part very wet ones, which makes the comparison of soil moisture between the models problematic.

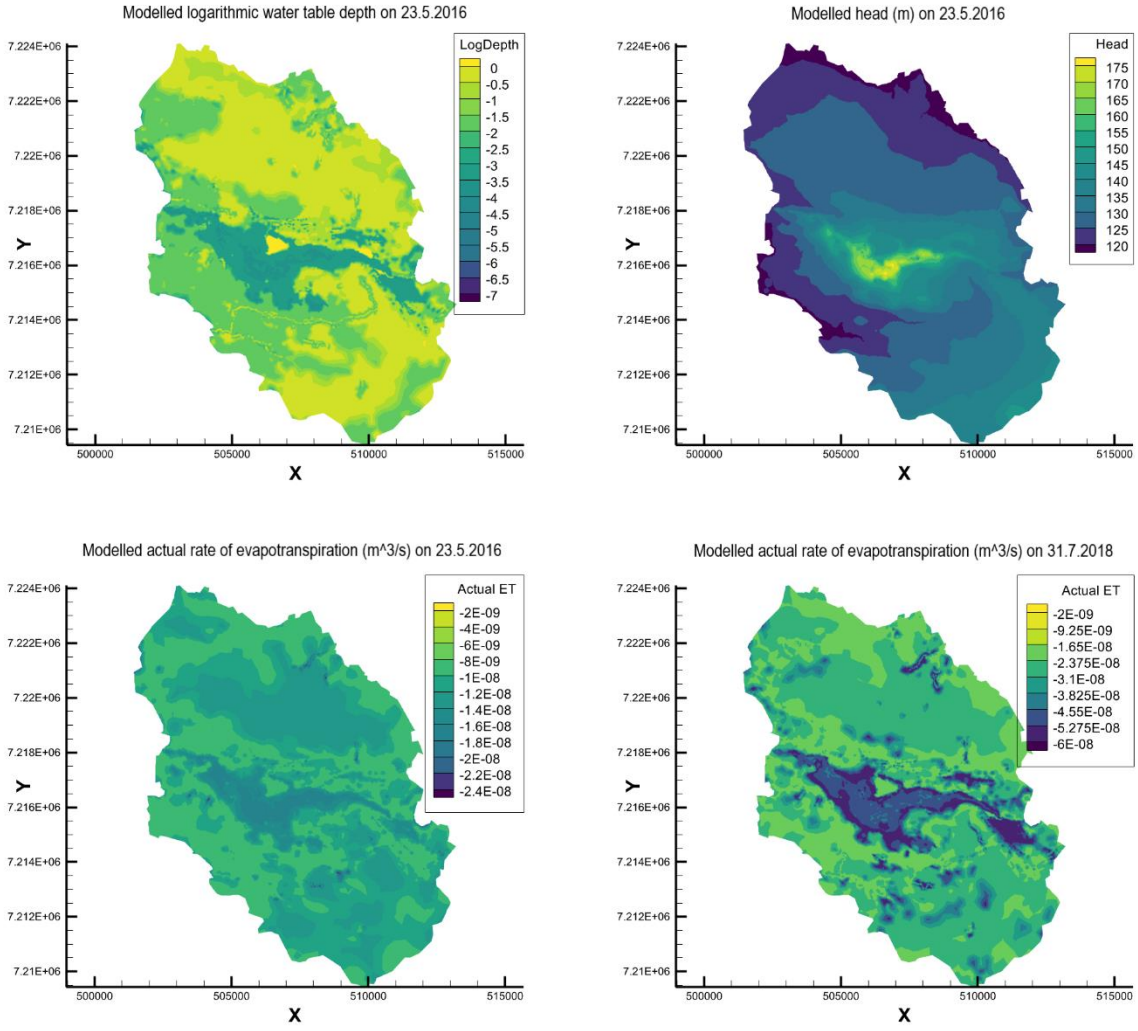

Figure 33. Examples of HGS model output maps (logarithmic water table, head, and rate of evapotranspiration) on the date when there was the most water table field observations (23.5.2016) and rate of evapotranspiration for a hot day (applied air temperature 24 °C) of 31.7.2018. The maps were created with Tecplot software. X and Y axles represent E and N coordinates in ETRS-TM35FIN coordinate system, respectively. Kälväsvaara aquifer is in the middle of the maps, and for example, the Lake Iso Kirkaslampi is clearly visible from the logarithmic water table depth map as a yellow spot on the northern premises of Kälväsvaara.

6 Conclusions

Although some wells performed better than others, the HGS model results revealed significant differences between simulated and observed values in most groundwater wells. Thus, HGS models need to be calibrated for better and more reliable results, but one may assume that they will perform better without calibration since most processes in HGS model are well described physically. Although most processes are physics based, they are extremely complex, require a lot of data, and it is nearly impossible to accurately represent all the small details and spatial differences in the entire model domain, thus emphasizing the importance of calibration and validation runs.

In contrast, the semi-distributed conceptual WSFS model performed considerably better because its parameters were fine-tuned over thousands of calibration runs. Calibration and validation of the WSFS model took time and produced satisfactory results, whereas in a highly discretized HGS model, fewer calibration runs would require more resources and time, making it harder to use in climate change and other scenario-based studies that require many runs. As opposed to conceptual models, HGS is largely physics-based; if parameters are well parameterized, it would perform much better than heavily calibrated semi-distributed conceptual WSFS model, which typically rely on the quality of the input observed data. In the case of full physically based models estimating parameter values can be challenging due to the large number of parameters required, as well as the long computational times.

Relatively simple models like the WSFS often fail to provide enough insight into the underlying physics, which makes it difficult to identify the errors they produce, especially in the absence of sufficient observed data. Furthermore, the HGS models can be used to solve almost any type of hydrological problem, whereas the WSFS has some limitations, including the inability to depict groundwater flow between subbasins (regional groundwater flow) and the failure to represent surface water (rivers and lakes) interactions with groundwater, to name a few. As a result, these are some of the areas in which the WSFS would aspire to improve in the future by incorporating the key hydrological processes via physics-based or by integrating other three-dimensional groundwater models (such as MODFLOW) into the WSFS to better understand the major hydrological processes, thus tracing model errors and improving results more effectively.

7 References

Ala-aho, P., Rossi, P. M., Isokangas, E., & Kløve, B. (2015). Fully integrated surface–subsurface flow modelling of groundwater–lake interaction in an esker aquifer: Model verification with stable isotopes and airborne thermal imaging. *Journal of Hydrology, 522*, 391-406. doi:https://doi.org/10.1016/j.jhydrol.2014.12.054

Ala-aho, P., Rossi, P. M., & Kløve, B. (2015). Estimation of temporal and spatial variations in groundwater recharge in unconfined sand aquifers using Scots pine inventories. *Hydrol. Earth Syst. Sci., 19*(4), 1961-1976. doi:10.5194/hess-19-1961-2015

Allen, R. G., Pereira, L. S., Raes, D., & Smith, M. (1998). Crop evapotranspiration-Guidelines for computing crop water requirements-FAO Irrigation and drainage paper 56. *Fao, Rome, 300*(9), D05109.

Aquanty. (2015). HydroGeoSphere User Manual. Release 1.0. In: Aquanty Inc. Waterloo.

Bergström, S. (1976). *Development and application of a conceptual runoff model for Scandinavian catchments*.

Brunner, P., & Simmons, C. T. (2012). HydroGeoSphere: A Fully Integrated, Physically Based Hydrological Model. *Groundwater, 50*(2), 170-176. doi:https://doi.org/10.1111/j.1745-6584.2011.00882.x

Devia, G. K., Ganasri, B. P., & Dwarakish, G. S. (2015). A Review on Hydrological Models. *Aquatic Procedia, 4*, 1001-1007. doi:https://doi.org/10.1016/j.aqpro.2015.02.126

Graham, D. N., & Butts, M. B. (2005). Flexible, integrated watershed modelling with MIKE SHE. *Watershed models, 849336090*, 245-272.

Gui, H., Wu, Z., & Zhang, C. (2021). Comparative Study of Different Types of Hydrological Models Applied to Hydrological Simulation. *CLEAN – Soil, Air, Water, 49*(8), 2000381. doi:https://doi.org/10.1002/clen.202000381

Heikkilä, H., & Lindholm, T. (1997). *Soiden ennallistamistutkimus vuosina 1987-1996*: Metsähallitus, luonnonsuojelu.

Heikkilä, R., Lindholm, T., & Tahvanainen, T. (2006). Mires of Finland–Daughters of the Baltic Sea.

Huttunen, I., Huttunen, M., Piirainen, V., Korppoo, M., Lepistö, A., Räike, A., . . . Vehviläinen, B. (2016). A national-scale nutrient loading model for Finnish watersheds—VEMALA. *Environmental Modeling & Assessment, 21*(1), 83-109.

Härkönen, S., Lehtonen, A., Manninen, T., Tuominen, S., & Peltoniemi, M. (2015). Estimating forest leaf area index using satellite images: comparison of k-NN based Landsat-NFI LAI with MODIS-RSR based LAI product for Finland.

Isokangas, E., Rossi, P. M., Ronkanen, A.-K., Marttila, H., Rozanski, K., & Kløve, B. (2017). Quantifying spatial groundwater dependence in peatlands through a distributed

isotope mass balance approach. *Water Resources Research, 53*(3), 2524-2541. doi:https://doi.org/10.1002/2016WR019661

Jakkila, J., Vento, T., Rousi, T., & Vehviläinen, B. (2013). SMOS soil moisture data validation in the Aurajoki watershed, Finland. *Hydrology Research, 45*(4-5), 684-702. doi:10.2166/nh.2013.234

Jaros, A., Rossi, P. M., Ronkanen, A.-K., & Kløve, B. (2019). Parameterisation of an integrated groundwater-surface water model for hydrological analysis of boreal aapa mire wetlands. *Journal of Hydrology, 575*, 175-191. doi:https://doi.org/10.1016/j.jhydrol.2019.04.094

Kontula, T., & Raunio, A. (2018). Suomen luontotyyppien uhanalaisuus 2018: Luontotyyppien punainen kirja. Osa 2: Luontotyyppien kuvaukset.

Li, Q., Unger, A., Sudicky, E., Kassenaar, D., Wexler, E., & Shikaze, S. (2008). Simulating the multi-seasonal response of a large-scale watershed with a 3D physically-based hydrologic model. *Journal of Hydrology, 357*(3-4), 317-336.

Neitsch, S. L., Arnold, J. G., Kiniry, J. R., & Williams, J. R. (2011). *Soil and water assessment tool theoretical documentation version 2009*. Retrieved from

Pechlivanidis, I., Jackson, B., Mcintyre, N., & Wheater, H. (2011). Catchment scale hydrological modelling: a review of model types, calibration approaches and uncertainty analysis methods in the context of recent developments in technology and applications. *Global NEST journal, 13*(3), 193-214.

Pirinen, P. (2021). 1 km x 1 km grind interpolated PET data for the years 2015-2020. Unpublished dataset (Accessed December 2021)

Rautiainen, M., Heiskanen, J., & Korhonen, L. (2012). Seasonal changes in canopy leaf area index and MODIS vegetation products for a boreal forest site in central Finland.

Räsänen, A., Juutinen, S., Kalacska, M., Aurela, M., Heikkinen, P., Mäenpää, K., . . . Virtanen, T. (2020). Peatland leaf-area index and biomass estimation with ultra-high resolution remote sensing. *GIScience & Remote Sensing, 57*(7), 943-964.

Seibert, J. (1997). Estimation of Parameter Uncertainty in the HBV Model: Paper presented at the Nordic Hydrological Conference (Akureyri, Iceland - August 1996). *Hydrology Research, 28*(4-5), 247-262. doi:10.2166/nh.1998.15

Similä, M., Aapala, K., & Penttinen, J. (2014). Ecological restoration in drained peatlands–best practices from Finland. Metsähallitus. *Finnish Environment Institute, Vantaa*.

Te Chow, V. (2010). *Applied hydrology*: Tata McGraw-Hill Education.

Vehviläinen, B. (1991). A physically based snowcover model. In *Recent Advances in the Modeling of Hydrologic Systems* (pp. 113-135): Springer.

Vehviläinen, B. (1992). *Snow cover models in operational watershed forecasting*: National Board of Waters and the Environment. Vesi-ja ympäristöhallitus.

Vehviläinen, B., & Huttunen, M. (2001) *Hydrological forecasting and real time monitoring in Finland: The watershed simulation and forecasting system (WSFS)*. Finnish Environment Institute, Helsinki, Finland.

Vehviläinen, B., & Huttunen, M. (2002). *The Finnish watershed simulation and forecasting system (WSFS).* Paper presented at the Publication of the 21st conference of Danube countries on the hydro-logical forecasting and hydrological bases of water management.